

WEAK LACUNAE OF ELECTROMAGNETIC WAVES IN DILUTE PLASMA*

S. V. TSYNKOV†

Abstract. The propagation of waves is said to be diffusionless, and the corresponding governing PDE (or system) is said to satisfy Huygens' principle if the waves due to compactly supported sources have sharp aft fronts. The areas of no disturbance behind the aft fronts are called lacunae. Diffusionless propagation of waves is rare, whereas its opposite—diffusive propagation accompanied by aftereffects—is common. Nonetheless, lacunae can still be observed in a number of important applications, including the Maxwell equations in vacuum or in dielectrics with static response. In the framework of these applications, lacunae can be efficiently exploited for the numerical simulation of unsteady waves, and considerable progress has been made toward the development of lacunae-based methods for computational electromagnetism. Maxwell equations in vacuum are Huygens' because they reduce to a set of d'Alembert equations. Besides d'Alembert equations, there are no other scalar Huygens' equations in the standard 3 + 1-dimensional Minkowski space-time. In terms of physics, this means that the mechanisms of dissipation and dispersion destroy the lacunae. In fact, all conventional low-frequency electromagnetic models, such as metals with Ohm conductivity, semiconductors, and magnetohydrodynamic media, are diffusive. An important case of the propagation of high-frequency electromagnetic waves in plasma is governed by the Klein–Gordon equation. It does not reduce to the d'Alembert equation either, and therefore the corresponding propagation is diffusive as well. However, one can still identify “weak lacunae” in the solutions of the Klein–Gordon equation, with the aft fronts that can be clearly observed, although they may not be as sharp as in the pure Huygens' case. Moreover, one can show that the “depth” of a weak lacuna is controlled by the dimensionless ratio of the Langmuir frequency to the primary carrying frequency of the waves.

Key words. Huygens' principle, wave diffusion, aftereffects, aft fronts, lacunae, ionospheric propagation, isotropic plasma, Langmuir frequency, cold plasma, transverse waves, Maxwell equations, Klein–Gordon equation, weak dispersion, short waves, external magnetic field, cyclotron frequency, gyrotropy, Faraday rotation

AMS subject classifications. 78A40, 35Q60, 81U30, 65Z05

DOI. 10.1137/060655134

1. Introduction.

1.1. The Huygens' principle. Consider a three-dimensional Cauchy problem for the wave (d'Alembert) equation:

$$(1.1) \quad \frac{1}{c^2} \frac{\partial^2 \varphi}{\partial t^2} - \Delta \varphi = f(\mathbf{x}, t), \quad \varphi(\mathbf{x}, 0) = \varphi_t(\mathbf{x}, 0) = 0,$$
$$\mathbb{R}^3 \ni \mathbf{x} = (x_1, x_2, x_3).$$

The fundamental solution of the d'Alembert operator is the expanding spherical wave (single layer)

$$(1.2) \quad \mathcal{E}(\mathbf{x}, t) = \frac{\Theta(t)}{4\pi} \frac{\delta(|\mathbf{x}| - ct)}{t},$$

*Received by the editors March 24, 2006; accepted for publication (in revised form) April 24, 2007; published electronically September 12, 2007. This research was supported by US Air Force grant FA9550-04-1-0118.

<http://www.siam.org/journals/siap/67-6/65513.html>

†Department of Mathematics, North Carolina State University, Box 8205, Raleigh, NC 27695 (tsynkov@math.ncsu.edu, <http://www4.ncsu.edu/~stsynkov>).

where $\Theta(t)$ is the Heaviside function, and the solution to the Cauchy problem (1.1) is given by the convolution of the fundamental solution (1.2) with the right-hand side $f(\mathbf{x}, t)$, i.e., by the Kirchhoff integral

$$(1.3) \quad \varphi(\mathbf{x}, t) = \mathcal{E} * f = \frac{1}{4\pi} \iiint_{\varrho \leq ct} \frac{f(\boldsymbol{\xi}, t - \varrho/c)}{\varrho} d\boldsymbol{\xi},$$

where $\mathbb{R}^3 \ni \boldsymbol{\xi} = (\xi_1, \xi_2, \xi_3)$ and $\varrho = |\mathbf{x} - \boldsymbol{\xi}|$.

Assume now that the right-hand side $f(\mathbf{x}, t)$ is compactly supported in space and in time, i.e., that $\text{supp } f \subseteq Q$, where Q is a bounded region in $\mathbb{R}^3 \times [0, +\infty) \equiv \{(\mathbf{x}, t) | \mathbf{x} \in \mathbb{R}^3, 0 \leq t < +\infty\}$. Then, the Kirchhoff formula (1.3) immediately implies that

$$(1.4) \quad \varphi(\mathbf{x}, t) \equiv 0 \quad \text{for } (\mathbf{x}, t) \in \bigcap_{(\boldsymbol{\xi}, \tau) \in Q} \{(\mathbf{x}, t) | |\mathbf{x} - \boldsymbol{\xi}| < c(t - \tau), t > \tau\}.$$

The region of space-time defined by formula (1.4) is known as the *lacuna* of the solution $\varphi(\mathbf{x}, t)$ of problem (1.1), because the solution vanishes there. This region can be interpreted as the intersection of all the characteristic cones of the d'Alembert equation, once the vertex of the cone sweeps the support Q of the right-hand side.

The presence of lacunae (or lacunas) in the solution is equivalent to the existence of the sharp aft fronts of the waves. In other words, the perturbation due to a compactly supported source first reaches a given fixed location of the observer and then ceases completely once a finite interval of time has elapsed. Subsequently, the solution at this location remains identically zero. Lacunae can then be viewed as areas of "quietness" behind the aft fronts, and the latter, reciprocally, serve as boundaries of the lacunae.

Differential equations, for which lacunae can be identified in their solutions, are said to satisfy *the Huygens' principle*. The most well-known classical example is provided by the foregoing d'Alembert equation. The Huygens' principle should not be confused with another concept that bears the same name and that often appears in the context of wave propagation in optics. Namely, according to *the Huygens' construction*, at every given moment of time the front of the propagating wave can be considered a collection of secondary sources that altogether define the wave field at subsequent moments of time [5].

Existence of the lacunae is a rare and fragile property. Its opposite is known as *the diffusion of waves* and is considered common. The diffusion manifests itself by aftereffects that accompany the propagation of waves governed by non-Huygens' equations. In this case, there are no sharp aft fronts, and once the perturbation has reached a given observation point it will never cease but only decay in amplitude.

A key constraint that distinguishes between the diffusionless and diffusive propagation is that lacunae may exist only *if the number of space dimensions is odd*. In particular, the propagation of waves governed by the d'Alembert equation on the plane (\mathbb{R}^2 , as opposed to \mathbb{R}^3) is already characterized by aftereffects.

Another important consideration is that studying the wave phenomena in the time domain is essential for the analysis and interpretation of the Huygens' principle. Indeed, a standard frequency-domain model is the Helmholtz equation

$$(1.5) \quad \Delta \hat{\varphi} + k^2 \hat{\varphi} = \hat{f},$$

which is obtained from the d'Alembert equation by applying the Fourier transform in time. In (1.5), $k^2 = \omega^2/c^2$, and $\hat{\varphi}$ denotes the complex amplitude of the time-harmonic

wave at the frequency ω (i.e., the ω Fourier coefficient). Solutions of the Helmholtz equation (1.5) are known to be analytic in the areas of homogeneity; therefore, they may not turn into zero only on a subdomain.

A review of the facts and publications in the literature pertaining to the Huygens' principle can be found in [3]; see also [10, 11]. The question of describing the hyperbolic differential equations and systems that admit the diffusionless propagation of waves was first formulated by Hadamard [12, 13, 14]. He did not know any other examples besides the classical d'Alembert equation. The notion of lacunae was introduced and studied by Petrowsky in [23]; see also [7, Chapter VI]. He obtained general conditions for the coefficients of hyperbolic equations/systems that guaranteed the presence of lacunae. Subsequent work in this direction was done by Atiyah, Bott, and Gårding in [1, 2]. However, no other constructive examples of lacunae in the solutions have been found besides solutions of the wave equation and its equivalents. In fact, Matthisson [20] has shown that in the standard 3 + 1-dimensional Minkowski space-time the only scalar hyperbolic equation that satisfies the Huygens' principle is the wave equation. From the standpoint of applications, this result provides one of the most convenient and useful criteria. Namely, the equation may be Huygens' only if it is equivalent to the d'Alembert equation. We will employ this criterion for the analysis in the current paper. In this regard, we also emphasize that the aforementioned equivalence does not have to be global; a given equation may only locally reduce to the d'Alembert equation. An interesting illustration of this fact is provided by Lax and Phillips in [19]—they analyze the waves that propagate on an n -dimensional sphere, where n is odd, and prove that the propagation is diffusionless. The first examples of nontrivial scalar equations (i.e., nonequivalent to the d'Alembert equation) that satisfy the Huygens' principle were built by Stellmacher (see [28, 16, 29]) in the spaces \mathbb{R}^n for odd $n \geq 5$. His examples have the form $c^{-2}\varphi_{tt} - \Delta\varphi + H(\mathbf{x}, t)\varphi = 0$, where the function $H(\mathbf{x}, t)$ is specially chosen to guarantee the diffusionless propagation, in which case it is called the Huygens' potential [3]. There are also examples of nontrivial diffusionless (i.e., Huygens') systems (as opposed to scalar equations) in the standard Minkowski 3 + 1 space-time [26, 3, 10], as well as examples of nontrivial scalar Huygens' equations in a 3 + 1-dimensional space-time but equipped with an alternative metric (the so-called plane wave metric); see [3, 10, 9].

1.2. Applications of lacunae. Lacunae of a given differential equation or system can be efficiently exploited for designing advanced numerical integration techniques. Lacunae-based methods have been developed previously for solving the scalar wave equation [25, 24], as well as for the problems of computational acoustics [31] and computational electromagnetism [32, 33, 34]. For the simplest possible setup that involves the radiation of waves by a known source, these methods guarantee that the grid convergence of a given discrete approximation will be *uniform in time*. For a more general setting that involves a sophisticated or potentially unknown mechanism of wave generation confined to a bounded region, lacunae-based methods facilitate construction of highly accurate unsteady artificial boundary conditions (ABCs) with only fixed and limited extent of temporal nonlocality in time. Note that overcoming the nonlocality of the exact unsteady ABCs in time has long been regarded as a challenging numerical issue [30]. From this perspective it is important to emphasize that the bound on temporal nonlocality obtained through the use of lacunae does not come at the expense of any approximation and/or simplification of the model; it is rather an implication of the fundamental properties of the corresponding solutions.

In addition to having the aforementioned computational benefits, lacunae can

also be instrumental in performing a number of tasks other than numerical ones. For example, explicit knowledge of their shape can help in planning of electromagnetic measurements and subsequent interpretation of the results.

In the current paper, we are not going to concentrate on numerical issues, except in section 3.5. Instead, we will focus on the phenomenon of lacunae itself. In particular, we will see that in the context of electromagnetism, only the simplest models that involve the propagation of waves in vacuum or in dielectrics with static response admit lacunae in the classical sense of the word. Many other traditional low-frequency models, such as different types of dielectrics, metals, semiconductors, magnetohydrodynamic media (MHD), turn out to be diffusive. However, for the important case of the propagation of high-frequency electromagnetic waves in dilute plasma, lacunae can still be identified in the solutions of the Maxwell equations in some approximate sense. Moreover, one can show that the quality, or “depth,” of these weak lacunae is controlled by the ratio of the Langmuir frequency, which is a key parameter that characterizes temporal responses of the plasma to the primary carrying frequency of the incident wave.

2. Traditional electromagnetic models.

2.1. The Maxwell system of equations. Lacunae in vacuum. The evolution of electromagnetic field in vacuum is governed by the classical Maxwell equations

$$(2.1) \quad \begin{aligned} \frac{1}{c} \frac{\partial \mathbf{B}}{\partial t} + \operatorname{curl} \mathbf{E} &= \mathbf{0}, & \operatorname{div} \mathbf{B} &= 0, \\ \frac{1}{c} \frac{\partial \mathbf{E}}{\partial t} - \operatorname{curl} \mathbf{B} &= -\frac{4\pi}{c} \mathbf{j}_{\text{ext}}, & \operatorname{div} \mathbf{E} &= 4\pi \rho_{\text{ext}}. \end{aligned}$$

In system (2.1), \mathbf{E} and \mathbf{B} are intensities of the electric and magnetic field, respectively, c is the speed of light, \mathbf{j}_{ext} is the density of the extraneous current, and ρ_{ext} is the density of the extraneous electric charge [17]. A *necessary solvability condition* for system (2.1) is continuity of the charges and currents:

$$(2.2) \quad \frac{\partial \rho_{\text{ext}}}{\partial t} + \operatorname{div} \mathbf{j}_{\text{ext}} = 0.$$

Equation (2.2) is obtained by taking divergence of the second unsteady equation of (2.1) and then substituting the second steady-state equation of (2.1). From the standpoint of physics, continuity (2.2) implies the conservation of electric charge. The rate of change of the total charge contained in any given region of space is equal to the flux of the charge, i.e., the total current, through the boundary of this region.

By differentiating each unsteady equation of (2.1) with respect to time, taking curl of the other unsteady equation, substituting $\operatorname{curl} \operatorname{curl}[\cdot] = \operatorname{grad} \operatorname{div}[\cdot] - \Delta[\cdot]$, and employing the corresponding steady-state equation of (2.1), we arrive at the following individual equations for the field intensities \mathbf{B} and \mathbf{E} :

$$(2.3) \quad \begin{aligned} \frac{1}{c^2} \frac{\partial^2 \mathbf{B}}{\partial t^2} - \Delta \mathbf{B} &= \frac{4\pi}{c} \operatorname{curl} \mathbf{j}_{\text{ext}}, \\ \frac{1}{c^2} \frac{\partial^2 \mathbf{E}}{\partial t^2} - \Delta \mathbf{E} &= -4\pi \left[\frac{1}{c^2} \frac{\partial \mathbf{j}_{\text{ext}}}{\partial t} + \operatorname{grad} \rho_{\text{ext}} \right]. \end{aligned}$$

Equations (2.3) are vector d’Alembert equations with the propagation speed c . Each equation of (2.3) is Huygens’ in \mathbb{R}^3 , and hence system (2.1) is also Huygens’. If the

charges ρ_{ext} and currents \mathbf{j}_{ext} are compactly supported, then the solution of (2.1) will have a lacuna of the same structure as determined by the Kirchhoff integral (1.3). Hence, the three-dimensional propagation of electromagnetic waves in vacuum is diffusionless.

Equations (2.1) will also remain a valid model for describing the electromagnetic field in various materials, but *only on the microscopic level*. The macroscopic equations are obtained by averaging; see [18]. In doing so, the impinging electromagnetic field may give rise to the induced charges and currents (see section 2.2), which, in turn, may affect the fields themselves. This range of phenomena is described by introducing the electric induction (or displacement) \mathbf{D} and the magnetic field \mathbf{H} , whereas the “old” quantity \mathbf{B} is referred to as the magnetic induction. The macroscopic Maxwell equations in the medium then become

$$(2.4) \quad \begin{aligned} \frac{1}{c} \frac{\partial \mathbf{B}}{\partial t} + \text{curl} \mathbf{E} &= \mathbf{0}, & \text{div} \mathbf{B} &= 0, \\ \frac{1}{c} \frac{\partial \mathbf{D}}{\partial t} - \text{curl} \mathbf{H} &= -\frac{4\pi}{c} \mathbf{j}_{\text{ext}}, & \text{div} \mathbf{D} &= 4\pi \rho_{\text{ext}}. \end{aligned}$$

Note that once \mathbf{B} is referred to as the induction, and \mathbf{H} as the magnetic field, system (2.4) looks mathematically more symmetric. However, as far as the physics is concerned, the true intensity of the magnetic field¹ is \mathbf{B} rather than \mathbf{H} . As for the right-hand sides' \mathbf{j}_{ext} and ρ_{ext} of system (2.4), they may be interpreted differently for different types of media and may sometimes be treated only as formal mathematical source terms.

System (2.4) is underdetermined unless additional relations are specified between the electric quantities \mathbf{E} and \mathbf{D} and the magnetic quantities \mathbf{H} and \mathbf{B} . These relations are determined by the medium, across which the electromagnetic waves propagate. They are called *the responses*. The responses may vary drastically for different types of media and different regimes of propagation. The simplest response is static.

2.2. Dielectric media with static response. Lacunae. A dielectric medium may not support a constant (i.e., steady-state) electric current. Responses of a dielectric medium can be characterized in terms of the electric polarization \mathbf{P} , which is the induced electric dipole moment per unit volume, and magnetization \mathbf{M} , which is the induced magnetic dipole moment per unit volume. Then, by definition,

$$(2.5) \quad \mathbf{D} = \mathbf{E} + 4\pi \mathbf{P} \quad \text{and} \quad \mathbf{B} = \mathbf{H} + 4\pi \mathbf{M}.$$

In an isotropic dielectric with static response, the electric induction \mathbf{D} is assumed directly proportional to the electric field \mathbf{E} , and the magnetic induction \mathbf{B} is assumed directly proportional to the magnetic field \mathbf{H} :

$$(2.6) \quad \mathbf{D} = \epsilon \mathbf{E} \quad \text{and} \quad \mathbf{B} = \mu \mathbf{H},$$

where the dielectric permittivity $\epsilon = \text{const}$ and the magnetic permeability $\mu = \text{const}$. In vacuum, we have $\epsilon = \mu = 1$, so that (2.4), (2.6) transform back to (2.1). In dielectric media other than vacuum, the assumptions of $\epsilon = \text{const}$ and $\mu = \text{const}$ may hold only for static incident fields. They can be used in the case of unsteady fields as well, but only as approximations and provided that *the incident frequencies*

¹A quantitative characteristic of the field that determines how it affects the moving charged particles.

are low,² i.e., considerably lower than the typical frequencies of the molecular or electronic oscillations that are responsible for the onset of electric polarization and/or magnetization of the medium.

Under the assumption of a static response (2.6), the Maxwell equations (2.4) reduce to

$$(2.7) \quad \begin{aligned} \frac{\mu}{c} \frac{\partial \mathbf{H}}{\partial t} + \operatorname{curl} \mathbf{E} &= \mathbf{0}, & \operatorname{div} \mathbf{H} &= 0, \\ \frac{\epsilon}{c} \frac{\partial \mathbf{E}}{\partial t} - \operatorname{curl} \mathbf{H} &= -\frac{4\pi}{c} \mathbf{j}_{\text{ext}}, & \operatorname{div} \mathbf{E} &= \frac{4\pi}{\epsilon} \rho_{\text{ext}}. \end{aligned}$$

Then, a procedure identical to the one used when deriving equations (2.3) from (2.1) yields

$$(2.8) \quad \begin{aligned} \frac{\epsilon\mu}{c^2} \frac{\partial^2 \mathbf{H}}{\partial t^2} - \Delta \mathbf{H} &= \frac{4\pi}{c} \operatorname{curl} \mathbf{j}_{\text{ext}}, \\ \frac{\epsilon\mu}{c^2} \frac{\partial^2 \mathbf{E}}{\partial t^2} - \Delta \mathbf{E} &= -4\pi \left[\frac{\mu}{c^2} \frac{\partial \mathbf{j}_{\text{ext}}}{\partial t} + \frac{1}{\epsilon} \operatorname{grad} \rho_{\text{ext}} \right]. \end{aligned}$$

Thus, equations (2.8) that individually govern the fields \mathbf{H} and \mathbf{E} in \mathbb{R}^3 are Huygens'. As such, so is system (2.7). The corresponding wave speed $c/\sqrt{\epsilon\mu}$ is slower than the speed of light c .

Unfortunately, the propagation in vacuum or in dielectrics with static response is practically the only case of electromagnetic propagation with no aftereffects. In sections 2.3, 2.4, and 2.5, we will see that many conventional electrodynamic models appear diffusive even before the onset of *dispersion*, i.e., for *low frequencies*, when static relations between \mathbf{D} , \mathbf{B} and \mathbf{E} , \mathbf{H} can still be employed for unsteady fields. The propagation remains diffusive in the case of higher incident frequencies as well.³

Note also that the description of the responses in terms of the polarization \mathbf{P} and magnetization \mathbf{M} (see (2.5)) naturally brings along the definition of the induced charge ρ_{ind} and the induced current \mathbf{j}_{ind} :

$$(2.9) \quad \rho_{\text{ind}} = -\operatorname{div} \mathbf{P}, \quad \mathbf{j}_{\text{ind}} = \frac{\partial \mathbf{P}}{\partial t} + c \operatorname{curl} \mathbf{M}.$$

Substitution of (2.5) and (2.9) into the Maxwell equations (2.4) yields

$$(2.10) \quad \begin{aligned} \frac{1}{c} \frac{\partial \mathbf{B}}{\partial t} + \operatorname{curl} \mathbf{E} &= \mathbf{0}, & \operatorname{div} \mathbf{B} &= 0, \\ \frac{1}{c} \frac{\partial \mathbf{E}}{\partial t} - \operatorname{curl} \mathbf{B} &= -\frac{4\pi}{c} (\mathbf{j}_{\text{ext}} + \mathbf{j}_{\text{ind}}), & \operatorname{div} \mathbf{E} &= 4\pi (\rho_{\text{ext}} + \rho_{\text{ind}}). \end{aligned}$$

System (2.10) is identical to (2.1), except that on its right-hand side we have the full current $\mathbf{j} = \mathbf{j}_{\text{ext}} + \mathbf{j}_{\text{ind}}$ and the full charge $\rho = \rho_{\text{ext}} + \rho_{\text{ind}}$ instead of only the extraneous quantities. This is an alternative way of representing the electromagnetic field inside a material—by looking at the actual intensities \mathbf{B} and \mathbf{E} only, but driven by the induced sources added to the original extraneous sources.⁴

²The notion of incident frequency is to be interpreted broadly here as frequency of any external excitation to the field inside the material, whether it be the frequency of the actual impinging wave or the frequency of the extraneous sources.

³Incident frequencies on the order of, or higher than, the characteristic microscopic frequencies for a given medium.

⁴Extraneous sources may or may not be present in every particular case.

2.3. Ohm conductivity in metals. In contradistinction to dielectrics, conducting materials can support a constant electric current. The steady-state model of a conductor can be obtained by dropping the displacement current $\frac{\partial \mathbf{D}}{\partial t} = \epsilon \frac{\partial \mathbf{E}}{\partial t}$ from the second unsteady Maxwell equation (2.4) or (2.7), which yields

$$(2.11) \quad \operatorname{curl} \mathbf{H} = \frac{4\pi}{c} \mathbf{j}_c.$$

The quantity \mathbf{j}_c on the right-hand side of (2.11) is called the conductivity current. In the pure static case it is assumed given, and then (2.11) is solved along with $\operatorname{div} \mathbf{B} = 0$ to determine the magnetic field. Note that according to formula (2.11) the conductivity current is solenoidal, $\operatorname{div} \mathbf{j}_c = 0$, which is a manifestation of the conservation of charge in this case.

The foregoing static model for conducting materials such as metals can also be applied to the analysis of slowly varying electromagnetic fields. In this case, however, the conductivity current \mathbf{j}_c shall no longer be treated as given. It rather becomes an unsteady current induced by the electric field that, in turn, is due to the variation in the magnetic field. Then, one also needs to add the first unsteady equation of the Maxwell system (2.4) or (2.7) to (2.11) and $\operatorname{div} \mathbf{B} = 0$. In doing so, the displacement current may still remain omitted from (2.11). The justification for not including it into the unsteady analysis is outlined in section 2.4, where a more comprehensive model is considered that includes semiconductors.

The key relation that one still needs in order to complete the unsteady model is a connection between the conductivity current and the electric field. Often, this connection is provided by the same classical Ohm law of electrostatics that establishes the direct proportionality between \mathbf{j}_c and the electric intensity \mathbf{E} :

$$(2.12) \quad \mathbf{j}_c = \sigma \mathbf{E}.$$

The quantity σ in formula (2.12) is the electric conductivity; in the isotropic case it is a scalar. The conductivity σ can be assumed constant, and accordingly, static relations (2.11), (2.12) can be used for the unsteady fields in metals, under conditions similar to those discussed in section 2.2. Namely, the frequency of the incident field must be much lower than the characteristic frequencies of the microscopic mechanism of conductivity, which is due to the collisions between the conductivity electrons and atoms of the crystal lattice. Therefore, the incident frequency must be much lower than the collision frequency $\mathcal{O}(v_e/\delta)$, where v_e is the electron thermal speed and δ is the mean free path.

By combining the first two equations of (2.4) with relations (2.11) and (2.12), we obtain the following system of equations that governs the unsteady electromagnetic field in metals:

$$(2.13) \quad \begin{aligned} \frac{1}{c} \frac{\partial \mathbf{B}}{\partial t} + \operatorname{curl} \mathbf{E} &= \mathbf{0}, & \operatorname{div} \mathbf{B} &= 0, \\ \operatorname{curl} \mathbf{H} &= \frac{4\pi}{c} \sigma \mathbf{E}, \end{aligned}$$

where we again assume that $\mathbf{B} = \mu \mathbf{H}$ with $\mu = \text{const}$. From system (2.13) we easily obtain

$$\frac{1}{c} \frac{\partial \mathbf{B}}{\partial t} + \operatorname{curl} \frac{c}{4\pi\sigma} \operatorname{curl} \mathbf{H} = \mathbf{0},$$

which, along with $\operatorname{div} \mathbf{B} = \mu \operatorname{div} \mathbf{H} = 0$, yields the following parabolic equation for the magnetic field \mathbf{H} :

$$(2.14) \quad \frac{\partial \mathbf{H}}{\partial t} - \frac{c^2}{4\pi\sigma\mu} \Delta \mathbf{H} = \mathbf{0}.$$

Once (2.14) is solved, the electric field \mathbf{E} is determined by the magnetic field through the last equation of (2.13). Equation (2.14) is not equivalent to the d'Alembert equation. Hence, according to the Matthiesson criterion [20], it is not Huygens', and there may be no lacunae in its solutions.

We should also notice that (2.14) is homogeneous and therefore may only be driven by the initial and/or boundary conditions, whereas previously we have analyzed lacunae in the solutions due to the compactly supported right-hand sides. Thus, let us see how a source term for (2.14) can be generated.

Let us introduce a nonphysical artificial current \mathbf{j}_a that will be included on the right-hand side of (2.11) and as such will be affecting the magnetic field \mathbf{H} ,

$$(2.15) \quad \operatorname{curl} \mathbf{H} = \frac{4\pi}{c} \mathbf{j}_c + \frac{4\pi}{c} \mathbf{j}_a,$$

but will not itself be driven by the induced electric field \mathbf{E} through the Ohm law (2.12). Then, we use (2.15) instead of (2.11) and obtain a modified form of system (2.13):

$$(2.16) \quad \begin{aligned} \frac{1}{c} \frac{\partial \mathbf{B}}{\partial t} + \operatorname{curl} \mathbf{E} &= \mathbf{0}, & \operatorname{div} \mathbf{B} &= 0, \\ \operatorname{curl} \mathbf{H} &= \frac{4\pi}{c} \sigma \mathbf{E} + \frac{4\pi}{c} \mathbf{j}_a. \end{aligned}$$

The conservation of charge in the case is expressed as the total current being solenoidal: $\operatorname{div}(\mathbf{j}_c + \mathbf{j}_a) = 0$. For simplicity, and with no substantial loss of generality (see Theorem 1 in [34]), we can also assume that the artificial current \mathbf{j}_a itself is divergence-free, $\operatorname{div} \mathbf{j}_a = 0$. In this case, the electric field will remain solenoidal as in system (2.13): $\operatorname{div} \mathbf{E} = 0$. From (2.16) we obtain the inhomogeneous counterpart of (2.14):

$$(2.17) \quad \frac{\partial \mathbf{H}}{\partial t} - \frac{c^2}{4\pi\sigma\mu} \Delta \mathbf{H} = \frac{1}{\sigma} \operatorname{curl} \mathbf{j}_a.$$

Solutions of (2.17) do not have lacunae even if \mathbf{j}_a is compactly supported. We can therefore conclude that the propagation of electromagnetic waves in the media with Ohm conductivity is diffusive.

2.4. Semiconductors. Let us now look more thoroughly into how one shall actually treat the displacement current for conducting materials. Keeping the unsteady term $\frac{1}{c} \frac{\partial \mathbf{D}}{\partial t} = \frac{\epsilon}{c} \frac{\partial \mathbf{E}}{\partial t}$, i.e., considering

$$(2.18) \quad \operatorname{curl} \mathbf{H} = \frac{4\pi}{c} \sigma \mathbf{E} - \frac{\epsilon}{c} \frac{\partial \mathbf{E}}{\partial t}$$

instead of (2.11), (2.12), can make sense only under the special circumstances when the second term on the right-hand side of (2.18) is of the same order of magnitude as the first term, or at least not negligibly small compared to the first term. If the field is time-harmonic, then the ratio of these two terms is $\mathcal{O}\left(\frac{\epsilon\omega}{4\pi\sigma}\right)$. In metals, we typically have $\frac{\omega}{\sigma} \ll 1$ for the entire range of frequencies, for which the conductivity σ can still be considered constant [18]. Therefore, (2.18) in metals indeed reduces to (2.13).

In semiconductors, however, because of the low concentration of conductivity electrons, the value of σ could be very small, so that for all those frequencies, for which σ and ϵ can still be regarded as constants, we may already have $\frac{\epsilon\omega}{4\pi\sigma} = \mathcal{O}(1)$. Then, the Maxwell equations become (cf. formulae (2.13) and (2.7))

$$(2.19) \quad \begin{aligned} \frac{\mu}{c} \frac{\partial \mathbf{H}}{\partial t} + \operatorname{curl} \mathbf{E} &= \mathbf{0}, & \operatorname{div} \mathbf{H} &= 0, \\ \frac{\epsilon}{c} \frac{\partial \mathbf{E}}{\partial t} + \frac{4\pi}{c} \sigma \mathbf{E} - \operatorname{curl} \mathbf{H} &= \mathbf{0}, & \operatorname{div} \mathbf{E} &= 0. \end{aligned}$$

By differentiating the second unsteady equation of (2.19) with respect to t , taking curl of the first unsteady equation, and then substituting $\operatorname{div} \mathbf{E} = 0$, we arrive at the telegrapher's equation for the electric field:

$$(2.20) \quad \frac{\epsilon\mu}{c^2} \frac{\partial^2 \mathbf{E}}{\partial t^2} + \frac{4\pi\mu\sigma}{c^2} \frac{\partial \mathbf{E}}{\partial t} - \Delta \mathbf{E} = \mathbf{0}.$$

A right-hand side for (2.20) can be built similarly to how it was done in section 2.3 for (2.14). Namely, if we were to formally add the artificial source terms $-\frac{4\pi}{c} \dot{\mathbf{j}}_a$ and $\frac{4\pi}{\epsilon} \rho_a$ to the second pair of the Maxwell equations (2.19), then we would have obtained the following equation instead of (2.20):

$$(2.21) \quad \frac{\epsilon\mu}{c^2} \frac{\partial^2 \mathbf{E}}{\partial t^2} + \frac{4\pi\mu\sigma}{c^2} \frac{\partial \mathbf{E}}{\partial t} - \Delta \mathbf{E} = -4\pi \left[\frac{\mu}{c^2} \frac{\partial \dot{\mathbf{j}}_a}{\partial t} + \frac{1}{\epsilon} \operatorname{grad} \rho_a \right].$$

The operator on the left-hand side of (2.21) is not equivalent to the d'Alembert operator. Therefore, the Huygens' principle will not hold, and there will be no lacunae. Note also that the larger the ratio $\frac{\epsilon\omega}{4\pi\sigma}$, the more of a standard dielectric behavior will be displayed by the medium governed by (2.18).

2.5. Magnetohydrodynamics. The case of a conducting medium in motion is not very different from the stationary conducting medium analyzed in section 2.3. Instead of the Ohm law (2.12) we now have

$$(2.22) \quad \mathbf{j}_c = \sigma \left(\mathbf{E} + \frac{1}{c} \mathbf{u} \times \mathbf{B} \right),$$

where \mathbf{u} denotes the velocity of the conducting fluid. The second term on the right-hand side of (2.22) is the so-called Lorentz correction that helps obtain the electric field in the frame of reference that moves with the velocity \mathbf{u} , provided that $|\mathbf{u}| \ll c$; see [17]. Accordingly, instead of system (2.13) we obtain

$$\begin{aligned} \frac{1}{c} \frac{\partial \mathbf{B}}{\partial t} + \operatorname{curl} \mathbf{E} &= \mathbf{0}, & \operatorname{div} \mathbf{B} &= 0, \\ \operatorname{curl} \mathbf{H} &= \frac{4\pi}{c} \sigma \left(\mathbf{E} + \frac{1}{c} \mathbf{u} \times \mathbf{B} \right), \end{aligned}$$

and instead of (2.14) we have

$$(2.23) \quad \frac{\partial \mathbf{H}}{\partial t} - \operatorname{curl}(\mathbf{u} \times \mathbf{H}) - \frac{c^2}{4\pi\sigma\mu} \Delta \mathbf{H} = \mathbf{0}.$$

As before, (2.23) is to be solved under the condition that the magnetic field is solenoidal: $\operatorname{div} \mathbf{H} = 0$.

Unlike in section 2.3, in magnetohydrodynamics the electromagnetic equations are not independent. They are coupled to the equations of the fluid flow through the quantity \mathbf{u} in (2.23). Moreover, the ponderomotive force $\frac{1}{c}\mathbf{j}_c \times \mathbf{H}$ is added to the right-hand side of the momentum equation of the fluid, and the Joule heat \mathbf{j}_c^2/σ is added to the right-hand side of the energy equation of the fluid. Therefore, we cannot directly apply the Matthisson criterion to (2.23); this can only be done if we consider the velocity field \mathbf{u} as given. Then, the answer is still negative—(2.23) is not Huygens’.

Of particular interest may be the case of very large (theoretically, infinite) conductivities σ , when the dissipative term $\sim \Delta \mathbf{H}$ can be dropped from (2.23). Let us then consider the equations of inviscid compressible flow coupled with (2.23) for the magnetic field with no magnetic viscosity, $\frac{c^2}{4\pi\sigma\mu} = 0$:

$$(2.24) \quad \begin{aligned} \frac{d\rho}{dt} + \rho \operatorname{div} \mathbf{u} &= 0, \\ \rho \frac{d\mathbf{u}}{dt} + \operatorname{grad} p &= \frac{1}{4\pi} \operatorname{curl} \mathbf{H} \times \mathbf{H}, \\ \frac{\partial \mathbf{H}}{\partial t} &= \operatorname{curl}(\mathbf{u} \times \mathbf{H}). \end{aligned}$$

In system (2.24), ρ , p , and T are the density, pressure, and temperature of the fluid, respectively, and $\frac{d}{dt} = \frac{\partial}{\partial t} + (\mathbf{u} \cdot \operatorname{grad})$. It is easy to show (see, e.g., [27, Vol. 1]) that infinite conductivity also implies the adiabatic nature of the flow, because the Joule heat $\frac{1}{\sigma}\mathbf{j}_c^2$ must be disregarded. Then, instead of the energy equation, system (2.24) can be supplemented by the Poisson adiabatic relation between the pressure and density of a thermodynamically ideal fluid: $p = \text{const} \cdot \rho^\gamma$, where $\gamma = \frac{c_p}{c_v}$ is the ratio of specific heats.

Let us linearize equations (2.24) at the background of an ambient conducting fluid immersed into a constant magnetic field, i.e., at the background of a constant solution: $\rho = \rho_0$, $p = p_0$, $\mathbf{u} = \mathbf{u}_0 = \mathbf{0}$, and $\mathbf{H} = \mathbf{H}_0$. Let $\rho = \rho_0 + \tilde{\rho}$, $p = p_0 + \tilde{p}$, $\mathbf{u} = \tilde{\mathbf{u}}$, and $\mathbf{H} = \mathbf{H}_0 + \tilde{\mathbf{H}}$, where all the quantities with the tilde are small perturbations. Retaining only the first order terms with respect to these perturbations, we obtain

$$\begin{aligned} \frac{\partial \tilde{\rho}}{\partial t} + \rho_0 \operatorname{div} \tilde{\mathbf{u}} &= 0, \\ \rho_0 \frac{\partial \tilde{\mathbf{u}}}{\partial t} + \operatorname{grad} \tilde{p} &= \frac{1}{4\pi} \operatorname{curl} \tilde{\mathbf{H}} \times \mathbf{H}_0, \\ \frac{\partial \tilde{\mathbf{H}}}{\partial t} &= \operatorname{curl}(\tilde{\mathbf{u}} \times \mathbf{H}_0), \\ \tilde{p} &= \frac{\gamma p_0}{\rho_0} \tilde{\rho}. \end{aligned}$$

Then, introducing the displacement vector \mathbf{x} as $\frac{\partial \mathbf{x}}{\partial t} = \tilde{\mathbf{u}}$, we can derive the following equation (see [15]):

$$(2.25) \quad \frac{\partial^2 \mathbf{x}}{\partial t^2} = c_s^2 \operatorname{grad} \operatorname{div} \mathbf{x} + c_A^2 \operatorname{grad}_\perp \operatorname{div} \mathbf{x}_\perp + c_A^2 \frac{\partial^2 \mathbf{x}_\perp}{\partial z^2},$$

where $c_s = \sqrt{\gamma p_0/\rho_0}$ is the conventional speed of sound, $c_A = |\mathbf{H}_0|/\sqrt{4\pi\rho_0}$ is the Alfvén speed, and \mathbf{x}_\perp and $\operatorname{grad}_\perp$ are the components of \mathbf{x} and the gradient, respectively, orthogonal to the magnetic field \mathbf{H}_0 .

For a particular class of transverse displacements, $\mathbf{x} = \mathbf{x}_\perp$ and $\text{div}\mathbf{x}_\perp = 0$, we obtain from (2.25)

$$(2.26) \quad \frac{\partial^2 \mathbf{x}_\perp}{\partial t^2} = c_A^2 \frac{\partial^2 \mathbf{x}_\perp}{\partial z^2}.$$

This is a one-dimensional d'Alembert equation that describes the propagation of the so-called Alfvén waves along the magnetic field with the speed c_A . Even though the number of space dimensions in (2.26) is odd, the one-dimensional case is special. Solutions to (2.26) may display the Huygens' behavior only if the equation is driven by some particular classes of initial data, whereas for the general RHS there is wave diffusion.

If the component of \mathbf{x} along the magnetic field \mathbf{H}_0 is not zero, i.e., $x_3 \neq 0$, then (2.25) yields

$$(2.27) \quad \frac{\partial^2 x_3}{\partial t^2} = c_s^2 \frac{\partial^2 x_3}{\partial z^2} + c_s^2 \frac{\partial}{\partial z} \text{div}\mathbf{x}_\perp.$$

For $\text{div}\mathbf{x}_\perp = 0$, (2.27) governs the propagation of the so-called ion sound along the magnetic field with the speed c_s . As in the previous case of the Alfvén waves, the propagation of ion sound is diffusive.

To supplement (2.27), a second equation can be derived from (2.25) that would govern $\text{div}\mathbf{x}_\perp$:

$$(2.28) \quad \begin{aligned} \frac{\partial^2 \text{div}\mathbf{x}_\perp}{\partial t^2} &= c_s^2 \text{divgrad}_\perp \underbrace{\text{div}\mathbf{x}}_{\text{div}\mathbf{x}_\perp + \frac{\partial x_3}{\partial z}} + c_A^2 \underbrace{\left[\text{divgrad}_\perp \text{div}\mathbf{x}_\perp + \frac{\partial^2 \text{div}\mathbf{x}_\perp}{\partial z^2} \right]}_{\Delta \text{div}\mathbf{x}_\perp} \\ &= c_s^2 \text{divgrad}_\perp \text{div}\mathbf{x}_\perp + c_s^2 \text{divgrad}_\perp \frac{\partial x_3}{\partial z} + c_A^2 \Delta \text{div}\mathbf{x}_\perp. \end{aligned}$$

Equations (2.27) and (2.28) form a system with the unknowns x_3 and $\text{div}\mathbf{x}_\perp$. These equations decouple only when $c_s \ll c_A$. In this case, the terms $\sim c_s^2$ on the right-hand side of (2.28) can be disregarded, which yields

$$(2.29) \quad \frac{\partial^2 \text{div}\mathbf{x}_\perp}{\partial t^2} = c_A^2 \Delta \text{div}\mathbf{x}_\perp.$$

Equation (2.29) governs the so-called magnetoacoustic waves that propagate with the Alfvén speed c_A . It is a true three-dimensional d'Alembert equation and as such, is Huygens'. The assumption of the speed of sound c_s being much slower than the Alfvén speed c_A holds when the thermodynamic pressure p_0 is much lower than the quantity $\mathbf{H}_0^2/8\pi$, which can be interpreted as pressure of the magnetic field [15].

Hence, lacunae can potentially exist in the solutions for the transverse quantity $\text{div}\mathbf{x}_\perp$. However, $\text{div}\mathbf{x}_\perp$ is then substituted into (2.27) to find the longitudinal displacement x_3 in magnetoacoustic waves, and the spatially one-dimensional solution for x_3 will, generally speaking, be diffusive. Altogether, the propagation of waves governed by (2.29), (2.27) will be only partially diffusionless.

2.6. Summary on low-frequency models. Having analyzed a number of conventional low-frequency electromagnetic models, we conclude that for most of them the propagation of waves is diffusive; i.e., the Huygens' principle does not hold. The driving frequency in these models is assumed lower than the characteristic microscopic frequencies of the medium, so that the material coefficients can be taken as constants

(permittivity, permeability, and conductivity). The mechanism that destroys the lacunae in all these cases is typically of a dissipative nature, related to the electric conductivity. An exception, for which the Huygens' principle holds, is pure dielectric materials with static response. Another partial exception is magnetoacoustic waves in the medium with infinite conductivity.

When the incident (driving) frequency becomes higher, the material coefficients can no longer be assumed constant. Instead, they become frequency-dependent, and while relations (2.6) can still keep their form, all the quantities involved have to be considered in the frequency domain rather than in the time domain. In other words, relations (2.6) transform into the corresponding relations between the Fourier coefficients of the fields and of material "constants," while in the physical space the medium responses typically appear nonlocal in time (given by convolution-type integrals); see [18]. It is also known that the discrepancy between \mathbf{H} and \mathbf{B} becomes unimportant/negligible even for relatively low frequencies. Hence, for higher frequencies only the discrepancy between \mathbf{D} and \mathbf{E} matters.

Hereafter, we will depart from the low-frequency framework and analyze the propagation of high-frequency electromagnetic waves in the dilute ionospheric plasma. We will see that in this case the key mechanism that can destroy the lacunae is of a dispersive nature. We will also see that under certain assumptions lacunae can still be identified in this dispersive medium, but in an approximate sense.

3. High-frequency electromagnetic waves in dilute plasma.

3.1. Characteristics of the medium. Our ultimate goal will be to work out an approximate interpretation of the Huygens' principle as it applies to the propagation of electromagnetic waves through the Earth's ionosphere. The ionosphere is a layer of dilute plasma (weakly ionized rarefied gas which is electrically neutral as a whole) surrounding the Earth at heights roughly between 60 km and 400 km from the surface. The primary source of ionization in the ionosphere is solar radiation. The negatively charged particles in the ionosphere are electrons with the charge of $e = -4.803 \cdot 10^{-10}$ Gaussian units and the mass of $m_e = 9.1 \cdot 10^{-28}g$, and the positively charged particles are ions that are much heavier: $m_i/m_e \gtrsim 2.93 \cdot 10^4$. The ionosphere is, in fact, layered, and its local parameters strongly depend on the altitude; this dependence for key characteristics, such as the concentrations of charged particles, may be nonmonotonic. The parameters of the ionosphere also change between day and night and winter and summer, and depend on the level of solar activity; more detail can be found, e.g., in [8, 6]. In our subsequent considerations, we will be quoting the parameters typical for the so-called F-layer (that starts at about 130 km above the Earth's surface) during the periods of low solar activity. The concentrations of the negatively and positively charged particles are equal, and we will mostly use the electron concentration: $n_e \approx 10^6 \text{ cm}^{-3}$. Note that the concentration of neutral atoms and molecules in the F-layer could be as high as $n_m = 10^{10} \text{ cm}^{-3}$. A typical value of the electron temperature in the F-layer is $T_e \approx 2000K$; the ions are a few times colder.

Several key quantities that depend on the foregoing parameters characterize the properties of the ionospheric plasma. The plasma electron frequency, also known as the Langmuir frequency, is defined as $\omega_{pe} = \sqrt{\frac{4\pi e^2 n_e}{m_e}}$; it provides a fundamental temporal scale. For the specific parameters of the plasma given above we obtain $\omega_{pe} \approx 5.64 \cdot 10^7 \text{ rad/s} \approx 9 \text{ MHz}$; in the literature, one can find the range of values for the Langmuir frequency in the ionosphere between 3 MHz and 15 MHz. The thermal speed of the electrons, $v_e = \sqrt{3\kappa T_e/2m_e} \approx 3 \cdot 10^7 \text{ cm/s}$, provides a characteristic

velocity, where $\kappa = 1.38 \cdot 10^{-16} \text{erg}/K$ is the Boltzmann constant; the speed v_e is roughly three orders of magnitude slower than the speed of light in vacuum, $c = 3 \cdot 10^{10}$ cm/s. The speed of the waves that propagate through the plasma will subsequently need to be compared to the characteristic velocity v_e . The Debye shielding length, $d = \sqrt{\frac{\kappa T_e}{8\pi e^2 n_e}} \approx 0.22$ cm, provides a characteristic spatial scale for the shielding of a point charge immersed into the plasma by other charges; shielding effectively results in multiplication of the classical Coulomb electrostatic potential by the rapidly decaying function $e^{-r/d}$.

Another important parameter yet to be included in the consideration is the magnetic field of the Earth, \mathbf{B}_0 , $|\mathbf{B}_0| \approx 0.3G$. It brings along another characteristic frequency known as the electron cyclotron frequency, $\Omega_e = \frac{e|\mathbf{B}_0|}{c \cdot m_e} \approx 0.8$ MHz, which is about an order of magnitude lower than the Langmuir frequency. The presence of \mathbf{B}_0 implies anisotropy of the plasma and transforms it into a gyrotropic medium; see [18]. The propagation of electromagnetic waves through such a medium is accompanied by interesting effects, e.g., the Faraday rotation. In the literature, these effects are typically studied in the frequency domain (see [18, Chapter XI]); for our analysis we will use the time domain (see section 3.6).

3.2. Cold plasma. In the Maxwell system of equations (2.10), assume that no extraneous charges or currents are present; then take curl of the first unsteady equation and by substitution eliminate the magnetic field from the second unsteady equation, having differentiated it with respect to time. This yields

$$(3.1) \quad \frac{\partial^2 \mathbf{E}}{\partial t^2} + c^2 \text{curlcurl} \mathbf{E} = -4\pi \frac{\partial \mathbf{j}_{\text{ind}}}{\partial t}.$$

Equation (3.1) is the key governing equation for the electric field. However, it still requires that the time derivative of the induced current on the right-hand side be specified. To do so, we will use the approximation known as cold plasma (see, e.g., [8, 21]); the meaning of the term will be explained later.

To obtain the current, let us write Newton's second law of motion for the electrons:

$$(3.2) \quad m_e \frac{d\mathbf{u}}{dt} + m_e \nu_{\text{eff}} \mathbf{u} = -e\mathbf{E} - \frac{e}{c} \mathbf{u} \times \mathbf{B}.$$

As the ions are much heavier than the electrons, their motion is not taken into account. In (3.2), \mathbf{u} denotes the velocity of the electrons due to the applied electromagnetic field (as opposed to the thermal velocity). Equation (3.2) is nonrelativistic because $\kappa T/m_e c^2 \approx 3.37 \cdot 10^{-7} \ll 1$. The quantity ν_{eff} in (3.2) is the effective frequency of collisions between the electrons and other particles (both charged and neutral). Note that the acceleration term in (3.2) is important in the case of high frequencies, whereas in the low-frequency case it is often omitted. Omitting the acceleration term results in (3.2) being transformed into the (generalized) Ohm law; see [15]. In the high-frequency case we can instead drop the collision term $m_e \nu_{\text{eff}} \mathbf{u}$ on the left-hand side of (3.2). This term is responsible for the mechanism of Ohm conductivity in the plasma and is dropped because typical collision frequencies ν_{eff} in the ionosphere are low. A thorough analysis of collisions in dilute plasma requires the calculation of cross-sections using the apparatus of quantum mechanics; it goes beyond the scope of this paper, and we refer the reader to [8]. Here we only mention that for the collisions of electrons with either positive ions or neutral molecules in the F-layer we have $\nu_{\text{eff}} \sim 10^2 s^{-1} \ll \omega_{pe}$, and as we are predominantly interested in high incident frequencies, $\omega \gg \omega_{pe}$, we can indeed disregard the collisions term in (3.2).

In the isotropic case, when the constant magnetic field \mathbf{B}_0 is not taken into account, the Lorentz term on the right-hand side of (3.2) can also be neglected. The reason is that unlike, for example, the case of MHD (section 2.5), when plasma is immersed into the magnetic field and the electric field is induced, here we are assuming that both the electric field and the magnetic field have roughly the same magnitude in the impinging wave. Then, the term $-\frac{e}{c}\mathbf{u} \times \mathbf{B}$ becomes a small relativistic correction, because $|\mathbf{u}| \ll c$. The latter relation always holds, because even when the plasma is not at thermal equilibrium, i.e., when the velocity distribution function is not Maxwellian, the speed of systematic motion $|\mathbf{u}|$ is still much slower than the average particle speed $\sqrt{2K/m_e e}$ (K is the kinetic energy), which, in turn, is much slower than the speed of light. Altogether, (3.2) then reduces to

$$(3.3) \quad m_e \frac{d\mathbf{u}}{dt} = -e\mathbf{E}.$$

Next, by expressing the induced current as $\mathbf{j}_{\text{ind}} = -en_e\mathbf{u}$, we transform (3.3) into

$$(3.4) \quad \frac{\partial \mathbf{j}_{\text{ind}}}{\partial t} = -en_e \frac{\partial \mathbf{u}}{\partial t} = \frac{e^2 n_e}{m_e} \mathbf{E}.$$

In doing so we note that the foregoing expression $\mathbf{j}_{\text{ind}} = -en_e\mathbf{u}$ corresponds to a simplified framework, whereas, strictly speaking, we should have written $\mathbf{j}_{\text{ind}} = -e \int \mathbf{v} f(\mathbf{v}) d\mathbf{v}$, where $f(\mathbf{v})$ is the probability distribution function for electron velocities. In this paper, however, we employ the elementary approach rather than the full-fledged kinetic considerations.

We would also like to emphasize that the relation (3.4) between the induced current and the electric field is local in space, because (3.3) is an ordinary differential equation. In the frequency domain, when all the variables are interpreted as Fourier components, we immediately have

$$\mathbf{j}_{\text{ind}}(\omega) = \frac{\omega_{\text{pe}}}{4\pi} \frac{1}{i\omega} \mathbf{E}(\omega),$$

and since $\frac{\partial \mathbf{D}}{\partial t} = \frac{\partial \mathbf{E}}{\partial t} + 4\pi \frac{\partial \mathbf{P}}{\partial t} = \frac{\partial \mathbf{E}}{\partial t} + 4\pi \mathbf{j}_{\text{ind}}$ (assuming $\mu = 1$; see (2.5), (2.9)), we obtain

$$(3.5) \quad \mathbf{D}(\omega) = \mathbf{E}(\omega) - \frac{\omega_{\text{pe}}^2}{\omega^2} \mathbf{E}(\omega) \stackrel{\text{def}}{=} \varepsilon \mathbf{E}(\omega) \quad \Rightarrow \quad \varepsilon = 1 - \frac{\omega_{\text{pe}}^2}{\omega^2}.$$

In other words, the electric permittivity ε depends only on the incident frequency ω and does not depend on the wavenumber \mathbf{k} . This is equivalent to neglecting the phenomenon of spatial dispersion in the plasma. It can indeed be neglected if $a \ll \lambda$, where a is a characteristic length and λ is the wavelength in the plasma. For the characteristic length we are taking the distance traveled by the electron during one period of fast oscillation, $a = 2\pi v_e/\omega$, and $\lambda = 2\pi v_{\text{ph}}/\omega = 2\pi/k$, where $k = |\mathbf{k}|$ and v_{ph} is the phase speed of the waves. Hence, we need to require that the phase speed be much faster than the thermal speed of the electrons:

$$(3.6) \quad v_{\text{ph}} = \frac{\omega}{k} \gg v_e = \sqrt{\frac{3\kappa T}{2m_e}},$$

which is also equivalent to requiring that $kd \ll \omega/\omega_{\text{pe}}$, where d is the Debye shielding length. The meaning of the term *cold plasma* can be explained with the help of

relation (3.6). Namely, the temperature should be sufficiently low so that the thermal speed is much slower than the phase speed of the waves.

Finally, by substituting expression (3.4) into the right-hand side of (3.1), we obtain

$$(3.7) \quad \frac{\partial^2 \mathbf{E}}{\partial t^2} + c^2 \operatorname{curl} \operatorname{curl} \mathbf{E} + \omega_{\text{pe}}^2 \mathbf{E} = \mathbf{0}.$$

Equation (3.7) is a self-contained governing equation for the electric field \mathbf{E} . It no longer includes any other unknown quantities that need to be determined through additional considerations. Equation (3.7) admits different types of propagating waves that we are going to analyze.

3.3. Longitudinal and transverse waves. According to the Helmholtz theorem (see [22, section 1.5]), any vector field has a unique representation as a sum of its irrotational (longitudinal) and solenoidal (transverse) components. In other words, we can write

$$(3.8) \quad \mathbf{E} = \mathbf{E}_{\parallel} + \mathbf{E}_{\perp}, \quad \text{where } \operatorname{curl} \mathbf{E}_{\parallel} = \mathbf{0} \quad \text{and} \quad \operatorname{div} \mathbf{E}_{\perp} = 0.$$

Note that calling the curl-free and divergence-free parts of the field by their alternative names—the longitudinal and transverse components, respectively—has a clear physical interpretation. Namely, in the frequency domain a plane wave propagating in an isotropic medium has the form $\mathbf{E} \sim e^{i\omega t + i\mathbf{k} \cdot \mathbf{r}}$, where \mathbf{r} is the radius vector. Then, clearly, $\operatorname{curl} \mathbf{E} \sim \mathbf{k} \times \mathbf{E}$ and $\operatorname{div} \mathbf{E} \sim \mathbf{k} \cdot \mathbf{E}$. As such, $\operatorname{curl} \mathbf{E}_{\parallel} = \mathbf{0}$ would mean that $\mathbf{k} \times \mathbf{E}_{\parallel} = \mathbf{0}$, or in other words, that \mathbf{E}_{\parallel} is parallel to the wave vector \mathbf{k} , which justifies its name of the longitudinal component. Similarly, $\operatorname{div} \mathbf{E}_{\perp} = 0$ would imply that $\mathbf{k} \cdot \mathbf{E}_{\perp} = 0$, or in other words, that \mathbf{E}_{\perp} is perpendicular to the wave vector \mathbf{k} , which justifies its name of the transverse component.

Let us consider the longitudinal waves first. In this case, (3.7) reduces to

$$(3.9) \quad \frac{\partial^2 \mathbf{E}_{\parallel}}{\partial t^2} + \omega_{\text{pe}}^2 \mathbf{E}_{\parallel} = \mathbf{0}.$$

Equation (3.9) governs the so-called Langmuir waves in plasma. As there is no spatial differentiation in (3.9), the Langmuir waves can basically be interpreted as high-frequency oscillations of the entire volume of plasma. The dispersion relation for the Langmuir waves is straightforward: $\omega^2 = \omega_{\text{pe}}^2$, which means that the oscillations always occur with one and the same frequency $\omega_{\text{pe}} = \sqrt{\frac{4\pi e^2 n_e}{m_e}}$. Accordingly, the group velocity of these waves is zero: $v_{\text{gr}} \stackrel{\text{def}}{=} \frac{\partial \omega}{\partial k} = 0$, which means that no energy transport is associated with the Langmuir waves.

On the other hand, propagation of the Langmuir waves is accompanied by perturbations of the local electric neutrality of the plasma. Indeed, according to the second steady-state Maxwell equation (2.10), when there are no extraneous charges we have

$$\rho_{\text{ind}} = \frac{1}{4\pi} \operatorname{div} \mathbf{E} = \frac{1}{4\pi} \operatorname{div} \mathbf{E}_{\parallel},$$

and, consequently, the density of the induced charge ρ_{ind} undergoes oscillations with the frequency ω_{pe} , because it is governed by the same differential equation as (3.9):

$$\frac{\partial^2 \rho_{\text{ind}}}{\partial t^2} + \omega_{\text{pe}}^2 \rho_{\text{ind}} = 0.$$

Let us reemphasize that the foregoing considerations are valid only when the phase velocity of the waves is large; see (3.6). By substituting $\omega = \omega_{pe}$ we obtain $v_{ph} = \omega_{pe}/k \gg \omega_{pe}d = v_e$, which means $kd \ll 1$, or in other words, the wavelength must be much greater than the Debye shielding length: $\lambda \gg d$. If this constraint does not hold, i.e., if $kd \sim 1$, then $v_{ph} \sim v_e$, and the assumption of cold plasma breaks down. In this case, the dispersion relation of the plasma can be obtained only by solving the kinetic equation. As shown, e.g., in [21, Chapter 13], the Langmuir waves become dispersive for slower phase speeds: $\omega^2 = \omega_{pe}^2 + 3k^2v_e^2$. Going even further down in the phase speed, i.e., allowing for $v_{ph} \ll v_e$, would necessitate taking the ions' motion into account; this leads to the ion sound that has been briefly discussed in section 2.5.

Having provided this very concise account of longitudinal oscillations, we will next turn to the primary subject of our discussion, the transverse high-frequency waves.

3.4. Transverse waves. To study the evolution of the transverse component \mathbf{E}_\perp of the electric field, we first notice that $\text{div} \mathbf{E}_\perp = 0$ implies $\text{curl} \text{curl} \mathbf{E}_\perp = -\Delta \mathbf{E}_\perp$, and, consequently, (3.7) transforms into the well-known Klein–Gordon equation

$$(3.10) \quad \frac{\partial^2 \mathbf{E}_\perp}{\partial t^2} - c^2 \Delta \mathbf{E}_\perp + \omega_{pe}^2 \mathbf{E}_\perp = \mathbf{0}.$$

The dispersion relation for the Klein–Gordon equation (3.10) is easy to obtain. It reads

$$(3.11) \quad \omega^2 = \omega_{pe}^2 + c^2 k^2,$$

which, in particular, means that similarly to the previous longitudinal case (see section 3.3), only high-frequency transverse waves can propagate in the plasma governed by (3.10). The range of allowable frequencies that corresponds to (3.11) is defined as $\omega > \omega_{pe}$.

From relation (3.11), one can easily obtain the phase speed and the group speeds of the waves:

$$(3.12) \quad v_{ph} = c \left(1 + \omega_{pe}^2 / c^2 k^2 \right)^{\frac{1}{2}} > c,$$

$$(3.13) \quad v_{gr} = c \left(1 + \omega_{pe}^2 / c^2 k^2 \right)^{-\frac{1}{2}} < c.$$

Unlike in the longitudinal case of section 3.3, the propagation of transverse waves preserves the local electric neutrality of the plasma, because $\text{div} \mathbf{E}_\perp = 0$. Moreover, it is possible to show (see [21, Chapter 13]), that even if one employs kinetic considerations for the analysis of transverse waves with a slow phase speed, $\omega/k \ll v_e$, there will, in fact, be no such waves. In other words, there are no thermal transverse modes analogous to the thermal longitudinal modes.

The dispersion properties of high-frequency transverse waves are of particular interest. Let us first assume that $\frac{\omega_{pe}}{ck} = \frac{v_e}{ckd} \ll 1$, which implies that $kd \gg \frac{v_e}{c} \approx 10^{-3}$, or in other words, that the waves are short: $\lambda \ll 10^3 d$, with the wavelength much shorter than a thousand times the Debye shielding length. These waves exhibit

a weakly dispersive behavior, as substitution of $\frac{\omega_{pe}}{ck} \ll 1$ into (3.12) and (3.13) immediately yields

$$(3.14) \quad v_{ph} \approx c \left(1 + \frac{\omega_{pe}^2}{2c^2 k^2} \right),$$

$$(3.15) \quad v_{gr} \approx c \left(1 - \frac{\omega_{pe}^2}{2c^2 k^2} \right).$$

We indeed see that both the phase speed v_{ph} of (3.14) and the group speed v_{gr} of (3.15) are close to the speed of light c , with the former being slightly faster than c and the latter being slightly slower than c . The frequency in this case, according to (3.11), is approximately equal to the speed of light times the wavenumber ($\omega \approx ck \gg \omega_{pe}$), and is also much higher than the Langmuir frequency. Note that the ultimate case of $v_{ph} = v_{gr} = c$, $\omega = ck$, would correspond to the propagation of waves with no dispersion in the framework of a pure d'Alembert equation rather than the Klein–Gordon equation.

In contradistinction to the short waves, the long transverse waves governed by (3.10) are similar to the longitudinal waves. Indeed, let $\frac{\omega_{pe}}{ck} \gg 1$; it means that $\lambda \gg 10^3 d$ and also that $\omega \gtrsim \omega_{pe}$, i.e., that the waves propagate with the frequencies close to the lowest possible frequency ω_{pe} . In this case, $v_{ph} \approx \omega_{pe}/k$, and $v_{gr} = c \cdot \frac{ck}{\omega_{pe}} \ll c$; i.e., the expression for the phase velocity is basically the same as that in the longitudinal case (see section 3.3), while the group velocity is small (in the pure longitudinal case it is equal to zero). This behavior is not surprising because the longer the wave, the less of a spatial variation per unit length it undergoes, and, consequently, the more the corresponding oscillations should resemble the oscillations of the entire plasma volume as a whole, which are characteristic of the longitudinal case.

In general, we should mention that the foregoing dispersion properties, while not completely unparalled, are, perhaps, still less typical than the inverse situation, when the long waves, rather than the short waves, exhibit a weakly dispersive behavior; see [15]. Our primary goal, however, is to see what can be said about the lacunae and the Huygens' principle for the waves governed by (3.10). From the previous considerations we conclude that *it is for the short waves, which are only weakly dispersive, that one can possibly observe some sort of "lacunae" in the solutions of (3.10)*. Indeed, in this case the propagation speeds (3.12) and (3.13) (see also (3.14) and (3.15)) are close to the nondispersive propagation velocity c , and therefore one may expect to see relatively few aftereffects behind what would have been the sharp aft fronts in the genuine Huygens' case. To provide a somewhat more accurate yet still qualitative argument, let us consider the waves propagating from an instantaneous point source located at the origin. Given the distance to the source r and the moment of time t , one can easily see that only those waves that have the group velocity $v_{gr} = r/t$ can reach the location r precisely at the moment t . Using expression (3.13) for the group velocity, we obtain a formula for k as it depends on r and t :

$$(3.16) \quad k = \frac{\omega_{pe}}{c} \left(\frac{c^2 t^2}{r^2} - 1 \right)^{-\frac{1}{2}}.$$

We see that the wavenumbers are defined only inside the light cone $r \leq ct$. Formula (3.16) also indicates that for a given moment of time t , the larger the r , the larger the k .

In other words, the closer the value of r to ct , the shorter the wave that reaches this location at time t , and ultimately, for the purely nondispersive propagation $r = ct$ the wavelength $\lambda = 2\pi/k$ defined by (3.16) becomes equal to zero.

Let us now fix some large wavenumber $k_1 \gg \frac{\omega_{pe}}{c}$ and consider a wave packet propagating from the origin with the range of wavenumbers $k \geq k_1$. By noticing that the group velocity v_{gr} of (3.13) is a monotone increasing function of k , we conclude that the range of group velocities for this packet will be

$$c(1 + \omega_{pe}^2/c^2k_1^2)^{-\frac{1}{2}} \leq v_{gr} < c.$$

Therefore, at every given moment of time t we can easily estimate how wide this packet is going to be. The width of the packet can be thought of as the spatial extent of the “tail” behind the aft front $r = ct$:

$$(3.17) \quad \delta_{tail} = (c - \min_k v_{gr})t = c \left[1 - \left(1 + \frac{\omega_{pe}^2}{c^2k_1^2} \right)^{-\frac{1}{2}} \right] t \approx ct \cdot \frac{\omega_{pe}^2}{2c^2k_1^2}.$$

We see that the tail expands linearly with time and shrinks quadratically as the minimum borderline wavenumber k_1 for the packet increases. We also note that the short waves, as they are defined above, $k \gg \frac{\omega_{pe}}{c}$, propagate with high frequencies $\omega \approx ck \gg \omega_{pe}$. Therefore, we can equivalently reformulate our general expectation in terms of the frequency rather than the wavelength. Namely, we hope that lacunae could be approximately observed in the solutions of (3.10) for high frequencies $\omega \gg \omega_{pe}$, whereas the overall range of frequencies allowed by the dispersion relation (3.11) is $\omega > \omega_{pe}$. Using the dispersion relation (3.11), we can also recast estimate (3.17) for the width of the aftereffects region (the tail) as

$$(3.18) \quad \delta_{tail} \approx ct \cdot \frac{\omega_{pe}^2}{2\omega_1^2},$$

where $\omega_1^2 = \omega_{pe}^2 + c^2k_1^2$ is the minimum borderline frequency for the packet we are considering: $\omega \geq \omega_1 \gg \omega_{pe}$. We also note that the ratio of the Langmuir frequency over the driving frequency of the waves that appears in formula (3.18) is going to play a key role in our subsequent analysis.

Let us emphasize, however, that the entire discussion based on the dispersion relation (3.11) is basically conducted in the frequency domain. On the other hand, we have seen in section 1.1 that the frequency domain is inadequate for the analysis of lacunae and the Huygens’ principle. A time-domain analysis is needed in order to see how the Huygens’ principle can be interpreted for the weakly dispersive transverse waves governed by (3.10).

Consider a three-dimensional Cauchy problem for the inhomogeneous Klein–Gordon equation (cf. (1.1)):

$$(3.19) \quad \frac{\partial^2 \varphi}{\partial t^2} - c^2 \Delta \varphi + \omega_{pe}^2 \varphi = f(\mathbf{x}, t), \quad \varphi(\mathbf{x}, 0) = \varphi_t(\mathbf{x}, 0) = 0,$$

$$\mathbb{R}^3 \ni \mathbf{x} = (x_1, x_2, x_3).$$

Compared to the vector equation (3.10), the differential equation in (3.19) is scalar and may govern, e.g., one Cartesian component of the total field. The right-hand side $f(\mathbf{x}, t)$ may be due to the extraneous current.

The Klein–Gordon equation is obviously not equivalent to the d’Alembert equation, and therefore, according to the Matthiesson criterion [20], its solutions must be diffusive and may have no lacunae in the classical sense of the word. The discrepancy between the two equations is accounted for by the term $\omega_{\text{pe}}^2 \varphi$ in (3.10). This term is responsible for the onset of dispersion that ruins the lacunae. We still hope, though, that the behavior of solutions to (3.10) will be close to Huygens’ when the dispersion is weak. Therefore, while it is clear that the term $\omega_{\text{pe}}^2 \varphi$ in the Klein–Gordon equation may not be completely disregarded, we would nonetheless like to see when it can be legitimately classified as “small.” Note that it is not as straightforward as simply calling the coefficient ω_{pe}^2 small, because this coefficient is *not dimensionless*. As such, we would rather need to identify special classes of solutions $\varphi = \varphi(x, t)$, for which the entire term $\omega_{\text{pe}}^2 \varphi$ can be deemed small. The previous frequency-domain considerations suggest that this may be the case when a high driving frequency $\omega \gg \omega_{\text{pe}}$ is brought into the time-domain analysis.

The fundamental solution for the Klein–Gordon operator can be obtained in the closed form (see [4]):

$$(3.20) \quad \mathcal{E}(\mathbf{x}, t) = \underbrace{\frac{\Theta(t)}{2\pi c} \delta(\beta^2)}_{\mathcal{E}_1(\mathbf{x}, t)} - \underbrace{\frac{\omega_{\text{pe}}^2}{4\pi c^3} \Theta(t) \Theta(\beta^2) \frac{J_1(y)}{y}}_{\mathcal{E}_2(\mathbf{x}, t)},$$

where $\beta^2 = c^2 t^2 - |\mathbf{x}|^2$, $y = \frac{\omega_{\text{pe}}}{c} \beta$, $J_1(\cdot)$ is the Bessel function, and $\Theta(\cdot)$ denotes the Heaviside function, as before. The first term $\mathcal{E}_1(\mathbf{x}, t)$ on the right-hand side of formula (3.20) is the same as the fundamental solution of the d’Alembert operator; see (1.2). The second term $\mathcal{E}_2(\mathbf{x}, t)$ can be interpreted as a correction due to the presence of $\omega_{\text{pe}}^2 \varphi$ in (3.19). Accordingly, solution $\varphi = \varphi(\mathbf{x}, t)$ of the Cauchy problem (3.19) is given by the convolution

$$(3.21) \quad \varphi = \mathcal{E} * f = \mathcal{E}_1 * f - \mathcal{E}_2 * f = \varphi_1 - \varphi_2,$$

where the first term $\varphi_1 = \mathcal{E}_1 * f$ on the right-hand side of (3.21) is the Kirchhoff integral (cf. formula (1.3)), while the second term $\varphi_2 = \mathcal{E}_2 * f$ is basically what “contaminates” the lacuna. We are going to study the properties of exactly this contaminating term for a particular choice of f .

Namely, we will consider the following point excitation for problem (3.19):

$$(3.22) \quad f(\mathbf{x}, t) = \begin{cases} M \cdot \delta(\mathbf{x}) \cdot \sin(\omega t) \equiv \delta(\mathbf{x}) \tilde{f}(t), & 0 \leq t \leq T, \\ 0, & t < 0 \text{ and } t > T, \end{cases}$$

where $M > 0$ and $T > 0$ are two parameters and ω denotes the driving frequency. We will assume that the source (3.22) undergoes sufficiently many oscillations with frequency ω during the interval $0 \leq t \leq T$. At the same time, this interval still remains finite, which allows us to preserve the time-dependent nature of the problem rather than have it transformed into the frequency domain. Choosing the right-hand side $f(\mathbf{x}, t)$ of (3.19) in the form (3.22) enables us to perform a sufficiently straightforward analysis on one hand, and, on the other hand, it still allows us to illustrate the key phenomena of interest.

According to the definition of the fundamental solution (see (3.20)), we have

(3.23)

$$\begin{aligned}\varphi_2 &= \frac{\omega_{\text{pe}}^2}{4\pi c^3} \int_0^t \iiint_{|\mathbf{x}-\boldsymbol{\xi}|\leq c|t-\tau|} \frac{f(\boldsymbol{\xi}, \tau) J_1\left(\omega_{\text{pe}}\sqrt{(t-\tau)^2 - |\mathbf{x}-\boldsymbol{\xi}|^2/c^2}\right)}{\omega_{\text{pe}}\sqrt{(t-\tau)^2 - |\mathbf{x}-\boldsymbol{\xi}|^2/c^2}} d\boldsymbol{\xi} d\tau \\ &= \frac{\omega_{\text{pe}}^2}{4\pi c^3} \int_0^{T_1} \frac{\tilde{f}(\tau) J_1\left(\omega_{\text{pe}}\sqrt{(t-\tau)^2 - |\mathbf{x}|^2/c^2}\right)}{\omega_{\text{pe}}\sqrt{(t-\tau)^2 - |\mathbf{x}|^2/c^2}} d\tau = \frac{\omega_{\text{pe}}^2}{4\pi c^3} \int_0^{T_1} \frac{\tilde{f}(\tau) J_1(y)}{y} d\tau,\end{aligned}$$

where $T_1 = \min\{t - |\mathbf{x}|/c, T\}$, $y = y(\tau, t, \mathbf{x}) = \omega_{\text{pe}}\sqrt{(t-\tau)^2 - |\mathbf{x}|^2/c^2}$, and $\tilde{f}(\tau)$ denotes the temporal dependence of the source term (3.22): $\tilde{f}(\tau) = M \sin(\omega\tau)$. We will analyze the cases of small and large arguments y of the Bessel function J_1 in formula (3.24). Let us first note that if y is small, or more precisely, if $0 \leq y \leq \mu_1^{(2)}$, where $\mu_1^{(2)}$ is the first positive root of the Bessel function $J_2(y)$, then the function

$$G(y) \stackrel{\text{def}}{=} \frac{J_1(y)}{y}$$

is a monotone decreasing function of the argument y . Indeed, we have

$$G'(y) = \frac{d}{dy} \left[\frac{J_1(y)}{y} \right] = -\frac{J_2(y)}{y} \leq 0 \quad \text{if } y \in [0, \mu_1^{(2)}].$$

The inequality $0 \leq y \leq \mu_1^{(2)}$ implies a constraint on the maximum value of t . In the worst-case scenario— $\tau = 0$ and $|\mathbf{x}| = 0$ —this constraint reads

$$(3.24) \quad t \leq \mu_1^{(2)}/\omega_{\text{pe}} \equiv T_0,$$

and from here on we will require that the most conservative sufficient condition (3.24) hold in order to guarantee that the value of y be sufficiently small.

We also notice that the function $y = y(\tau, \cdot)$ is a monotone decreasing function of its argument τ on the interval $0 \leq \tau \leq T_1$. Consequently, the composite function $\tilde{G}(\tau) = G(y(\tau, \cdot))$ is a monotone increasing function of τ . We can then apply the Bonnet theorem (second mean value theorem) (see [35]), to the last integral from (3.24) and obtain

$$(3.25) \quad \varphi_2 = \frac{\omega_{\text{pe}}^2}{4\pi c^3} \left[\tilde{G}(0) \int_0^\eta \tilde{f}(\tau) d\tau + \tilde{G}(T_1) \int_\eta^{T_1} \tilde{f}(\tau) d\tau \right],$$

where η is some point of the interval $[0, T_1]$.

We note that the contaminating part φ_2 of the solution will eventually need to be compared against its regular part φ_1 , which, according to (1.3), is given by

$$(3.26) \quad \varphi_1(\mathbf{x}, t) = \frac{1}{4\pi c^2} \frac{\tilde{f}(t - |\mathbf{x}|/c)}{|\mathbf{x}|},$$

where, again, $\tilde{f}(t) = M \sin(\omega t)$ for $t \in [0, T]$; see (3.22). The function φ_1 of (3.26) represents a genuine d'Alembert wave packet due to the source (3.22); it may differ from zero only on the region $c(t - T) \leq |\mathbf{x}| \leq ct$. For $|\mathbf{x}| > ct$ we have $\varphi_1(\mathbf{x}, t) = 0$

because the propagation speed is finite, and for $|\mathbf{x}| < c(t - T)$ we have $\varphi_1(\mathbf{x}, t) = 0$ because this is a lacuna of the wave equation.

Similarly, for $|\mathbf{x}| > ct$ we also have $\varphi_2(\mathbf{x}, t) = 0$. However, otherwise $\varphi_2(\mathbf{x}, t) \neq 0$ either in the wave packet area $c(t - T) \leq |\mathbf{x}| \leq ct$ or in the lacuna area $|\mathbf{x}| < c(t - T)$. The wave packet area corresponds to $T_1 = (t - |\mathbf{x}|/c) \leq T$; then $y(T_1, \cdot) = 0$, and, consequently, $\tilde{G}(T_1) = G(0) = 1/2$ in formula (3.25). In contradistinction to that, the area that would have been a lacuna in the nondispersive case corresponds to $T_1 = T < t - |\mathbf{x}|/c$, which means $y(T_1, \cdot) = y(T, \cdot) > 0$ and $\tilde{G}(T_1) < 1/2$. Altogether, the constants in formula (3.25) can be estimated as follows (recall that $\mu_1^{(2)} \approx 5.13562230$):

$$(3.27) \quad -6.61397437 \cdot 10^{-2} = G(\mu_1^{(2)}) \leq \tilde{G}(0) < \tilde{G}(T_1) \leq G(0) = \frac{1}{2}.$$

By evaluating the integrals in (3.25), we obtain

$$(3.28) \quad \begin{aligned} \varphi_2 &= \frac{\omega_{pe} M}{4\pi c^3} \frac{\omega_{pe}}{\omega} \left[\tilde{G}(0) (1 - \cos(\omega\eta)) + \tilde{G}(T_1) (\cos(\omega\eta) - \cos(\omega T_1)) \right] \\ &= \frac{\omega_{pe} M}{4\pi c^3} \frac{\omega_{pe}}{\omega} \left[\tilde{G}(0) + (\tilde{G}(T_1) - \tilde{G}(0)) \cos(\omega\eta) - \tilde{G}(T_1) \cos(\omega T_1) \right], \end{aligned}$$

and according to estimates (3.27), the absolute value of the quantity in rectangular brackets in formula (3.28) may never exceed $3/2 - G(\mu_1^{(2)})$.

Let us now compare the dispersionless solution φ_1 of (3.26) with the dispersion-induced correction φ_2 of (3.28). Note that φ_1 is defined only inside the wave packet area, $c(t - T) \leq |\mathbf{x}| \leq ct$, including the aft front $|\mathbf{x}| = c(t - T)$. We can then recast formula (3.26) as

$$(3.29) \quad \varphi_1(\mathbf{x}, t) = \frac{M}{4\pi c^3} \frac{\sin(\omega T_1)}{t - T_1}$$

and thus obtain

$$(3.30) \quad \frac{\sup_{|\mathbf{x}| \leq ct} |\varphi_2(\mathbf{x}, t)|}{\sup_{c(t-T) \leq |\mathbf{x}| \leq ct} |\varphi_1(\mathbf{x}, t)|} = \left(\frac{3}{2} - G(\mu_1^{(2)}) \right) \omega_{pe} (t - T_1) \frac{\omega_{pe}}{\omega}.$$

In formula (3.29), we can always consider $\omega_{pe}(t - T_1) < \mu_1^{(2)}$ because of inequality (3.24). As such,

$$(3.31) \quad \frac{\sup |\varphi_2|}{\sup |\varphi_1|} = \mathcal{O} \left(\frac{\omega_{pe}}{\omega} \right).$$

Estimate (3.31) is important as it quantifies the previously outlined “tentative” consideration that the higher the driving frequency, the more of a lacuna one might be able to observe in the corresponding solution. It is because of this particular estimate (see (3.31)) that we can call the region $|\mathbf{x}| < c(t - T)$ for $t \leq T_0$ a *weak lacuna* and also refer to the quantity on the left-hand side of (3.31) as its “*depth*.” Indeed, the region $|\mathbf{x}| < c(t - T)$ corresponds to the genuine lacuna of the d’Alembert equation. In the dispersive case, there is still a residual field inside this region, but its magnitude relative to the magnitude of the field in the packet (the depth of a weak lacuna) is

small and, quantitatively, is proportional to the ratio of the Langmuir frequency over the driving frequency of the waves.

Next, we will consider the opposite case—that of the large argument y of the Bessel function J_1 in formula (3.24). Our goal will be to justify a relation similar to (3.31) for long propagation times.

Let $y \gg 1$. Then, we will use the asymptotic form of the Bessel function $J_1(y)$,

$$(3.32) \quad J_1(y) = \sqrt{\frac{2}{\pi y}} \cos\left(y - \frac{3\pi}{4}\right) + \mathcal{O}\left(y^{-\frac{3}{2}}\right),$$

which means that by disregarding the higher order terms $\mathcal{O}(y^{-\frac{5}{2}})$ in the integral (3.24) we can recast it as

$$(3.33) \quad \varphi_2 \approx \frac{\omega_{pe}^2}{4\pi c^3} \sqrt{\frac{2}{\pi}} \int_0^{T_1} \tilde{f}(\tau) y^{-\frac{3}{2}} \cos\left(y - \frac{3\pi}{4}\right) d\tau.$$

We would like to estimate the magnitude of $\varphi_2(\mathbf{x}, t)$ of (3.33) for $|\mathbf{x}| < c(t - T)$, i.e., inside the region that would have been a lacuna in the nondispersive case. This means that the upper integration limit in formula (3.33) can be taken as $T_1 = T$.

Let us first analyze the expression for $y = y(\tau, t, \mathbf{x}) = \omega_{pe} \sqrt{(t - \tau)^2 - |\mathbf{x}|^2/c^2}$ that enters into formulae (3.32) and (3.33) and see under what conditions it can indeed be regarded as large. Obviously, as $\tau \in [0, T]$, then $\min_{\tau} y(\tau, t, \mathbf{x}) = y(T, t, \mathbf{x})$, and it will be sufficient to see when $y(T, t, \mathbf{x})$ is large. To begin with, we notice that for a given moment of time t , the quantity $y(T, t, \mathbf{x})$ cannot be large all across the lacuna, because on the aft front $|\mathbf{x}| = c(t - T)$ we have $y(T, t, c(t - T)) = 0$. Consequently, to be able to legitimately use the asymptotics (3.32) we will need to step inside the lacuna.

Then we introduce the distance δ between a given point inside the lacuna and the aft front at the moment of time, t . For $|\mathbf{x}| = c(t - T) - \delta$ we have $y = \frac{\omega_{pe}}{c} \sqrt{2c(t - T)\delta - \delta^2}$. We can therefore conclude that if we consider δ as a function of time, $\delta = \delta(t)$, and require that

$$\lim_{t \rightarrow \infty} [2c(t - T) \cdot \delta(t) - \delta^2(t)] = \infty,$$

then the quantity $y = y(T, t, \mathbf{x})$ will increase with no bound when $t \rightarrow \infty$ and $|\mathbf{x}| \leq c(t - T) - \delta(t)$. Clearly, in so doing the “gap width” δ itself may even decrease as t increases, but only more slowly than $(t - T)^{-1}$. On the other hand, δ may also be a constant or an increasing function of the argument t ; in the latter case it may not increase faster than linearly because the lacuna itself expands only linearly with respect to time.

To summarize, we can claim that

$$\lim_{t \rightarrow \infty} y(T, t, \mathbf{x}) = \infty$$

uniformly for all \mathbf{x} such that $|\mathbf{x}| \leq c(t - T) - \delta(t)$, provided that

$$(3.34) \quad \frac{\text{const}}{(t - T)\zeta(t)} \leq \delta(t) \leq (c - c_1)(t - T),$$

where $c_1 < c$ and $\zeta(t)$ is an auxiliary function such that $\zeta(t) = o(1)$ as $t \rightarrow \infty$. Clearly, the most conservative strategy for choosing the gap width, $\delta = (c - c_1)(t - T)$,

where $c_1 < c$, will guarantee the fastest growth of y in a narrower cone $|\mathbf{x}| < c_1(t-T)$:

$$(3.35) \quad \forall \mathbf{x} : |\mathbf{x}| \leq c_1(t-T), \quad c_1 < c \quad \& \quad \forall \tau \in [0, T] : \\ y(\tau, t, \mathbf{x}) \geq y(T, t, \mathbf{x}) \geq \omega_{\text{pe}} \sqrt{1 - c_1^2/c^2} (t-T).$$

Estimate (3.35) will allow us to use the asymptotic formulae (3.32) and (3.33) for sufficiently large times t .

Next, we notice that $y^{-\frac{3}{2}}$ is a monotone decreasing function of y for $y > 0$, and as $y = y(\tau, t, \mathbf{x})$ is, in turn, a monotone decreasing function of τ for $\tau \in [0, T]$, it follows that $y^{-\frac{3}{2}}$ is a monotone increasing function of τ . Consequently, we can apply the Bonnet theorem again, this time to the integral (3.33), and obtain (recall that $T_1 = T$ for the interior of the lacuna)

$$(3.36) \quad \varphi_2 \approx \frac{\omega_{\text{pe}}^2}{4\pi c^3} \sqrt{\frac{2}{\pi}} \left[(y(0, t, \mathbf{x}))^{-\frac{3}{2}} \int_0^\eta \tilde{f}(\tau) \cos\left(y(\tau, t, \mathbf{x}) - \frac{3\pi}{4}\right) d\tau \right. \\ \left. + (y(T, t, \mathbf{x}))^{-\frac{3}{2}} \int_\eta^T \tilde{f}(\tau) \cos\left(y(\tau, t, \mathbf{x}) - \frac{3\pi}{4}\right) d\tau \right],$$

where $\eta \in [0, T]$. Let us now substitute $\tilde{f}(\tau) = M \sin(\omega\tau)$ into (3.36):

$$\varphi_2 \approx \frac{M\omega_{\text{pe}}^2}{8\pi c^3} \sqrt{\frac{2}{\pi}} \left[(y(0, t, \mathbf{x}))^{-\frac{3}{2}} \int_0^\eta \left\{ \sin\left(\omega\tau + y(\tau, t, \mathbf{x}) - \frac{3\pi}{4}\right) \right. \right. \\ \left. \left. - \sin\left(\omega\tau - y(\tau, t, \mathbf{x}) + \frac{3\pi}{4}\right) \right\} d\tau \right. \\ \left. + (y(T, t, \mathbf{x}))^{-\frac{3}{2}} \int_\eta^T \left\{ \sin\left(\omega\tau + y(\tau, t, \mathbf{x}) - \frac{3\pi}{4}\right) \right. \right. \\ \left. \left. - \sin\left(\omega\tau - y(\tau, t, \mathbf{x}) + \frac{3\pi}{4}\right) \right\} d\tau \right].$$

The argument $(\omega\tau \pm y(\tau, t, \mathbf{x}) \mp \frac{3\pi}{4})$ of the sine functions above can be approximated as follows. Denote $\nu = T - \tau$, $0 \leq \nu \leq T$, and recast y in the form

$$(3.37) \quad y(\tau, t, \mathbf{x}) = \omega_{\text{pe}} \sqrt{(t-T)^2 - |\mathbf{x}|^2/c^2} \sqrt{1 + \frac{2(t-T)\nu + \nu^2}{(t-T)^2 - |\mathbf{x}|^2/c^2}}.$$

Notice that if

$$\frac{2(t-T)\nu}{(t-T)^2 - \frac{|\mathbf{x}|^2}{c^2}} = \frac{2\nu}{(t-T) \left(1 - \frac{|\mathbf{x}|^2}{(t-T)^2 c^2}\right)} \ll 1,$$

then also

$$\frac{\nu^2}{(t-T)^2 - \frac{|\mathbf{x}|^2}{c^2}} = \frac{\nu^2}{(t-T)^2 \left(1 - \frac{|\mathbf{x}|^2}{(t-T)^2 c^2}\right)} \\ = \left[\frac{\nu}{(t-T) \left(1 - \frac{|\mathbf{x}|^2}{(t-T)^2 c^2}\right)} \right]^2 \left(1 - \frac{|\mathbf{x}|^2}{(t-T)^2 c^2}\right) \ll 1.$$

Consequently, if the linear term with respect to ν under the second square root in formula (3.37) is indeed small, then the quadratic term can be disregarded, which yields

$$y(\tau, t, \mathbf{x}) \approx y(T, t, \mathbf{x}) + \frac{\omega_{\text{pe}}^2(t-T)\nu}{y(T, t, \mathbf{x})} = \underbrace{y(T, t, \mathbf{x}) + \frac{\omega_{\text{pe}}^2(t-T)T}{y(T, t, \mathbf{x})}}_{\text{does not depend on } \tau} - \frac{\omega_{\text{pe}}^2(t-T)\tau}{y(T, t, \mathbf{x})}.$$

Therefore, we can write

$$\begin{aligned} \varphi_2 \approx & \frac{M\omega_{\text{pe}}^2}{8\pi c^3} \sqrt{\frac{2}{\pi}} \left[(y(0, t, \mathbf{x}))^{-\frac{3}{2}} \int_0^\eta \left\{ \sin((\omega + \gamma\omega_{\text{pe}})\tau - \alpha) \right. \right. \\ & \left. \left. - \sin((\omega + \gamma\omega_{\text{pe}})\tau - \alpha) \right\} d\tau \right. \\ & \left. + (y(T, t, \mathbf{x}))^{-\frac{3}{2}} \int_\eta^T \left\{ \sin((\omega - \gamma\omega_{\text{pe}})\tau + \alpha) \right. \right. \\ & \left. \left. - \sin((\omega + \gamma\omega_{\text{pe}})\tau - \alpha) \right\} d\tau \right], \end{aligned}$$

where $\gamma = \frac{\omega_{\text{pe}}(t-T)}{y(T, t, \mathbf{x})}$ and $\alpha = y(T, t, \mathbf{x}) + \frac{\omega_{\text{pe}}^2(t-T)T}{y(T, t, \mathbf{x})} - \frac{3\pi}{4}$. The integrals can now be explicitly evaluated:

$$\begin{aligned} \varphi_2 \approx & \frac{M\omega_{\text{pe}}^2}{8\pi c^3} \sqrt{\frac{2}{\pi}} \left[(y(0, t, \mathbf{x}))^{-\frac{3}{2}} \left\{ \frac{\cos \alpha - \cos((\omega - \gamma\omega_{\text{pe}})\eta + \alpha)}{\omega - \gamma\omega_{\text{pe}}} \right. \right. \\ & \left. \left. - \frac{\cos \alpha - \cos((\omega + \gamma\omega_{\text{pe}})\eta - \alpha)}{\omega + \gamma\omega_{\text{pe}}} \right\} \right. \\ & \left. + (y(T, t, \mathbf{x}))^{-\frac{3}{2}} \left\{ \frac{\cos((\omega - \gamma\omega_{\text{pe}})\eta + \alpha) - \cos((\omega - \gamma\omega_{\text{pe}})T + \alpha)}{\omega - \gamma\omega_{\text{pe}}} \right. \right. \\ & \left. \left. - \frac{\cos((\omega + \gamma\omega_{\text{pe}})\eta - \alpha) - \cos((\omega + \gamma\omega_{\text{pe}})T - \alpha)}{\omega + \gamma\omega_{\text{pe}}} \right\} \right], \end{aligned}$$

and using (3.35) we obtain

$$\begin{aligned} |\varphi_2(\mathbf{x}, t)| & \leq \frac{M\omega_{\text{pe}}^2}{4\pi c^3} \sqrt{\frac{2}{\pi}} \left[(y(0, t, \mathbf{x}))^{-\frac{3}{2}} + (y(T, t, \mathbf{x}))^{-\frac{3}{2}} \right] \\ & \quad \cdot \left\{ \frac{1}{\omega - \gamma\omega_{\text{pe}}} + \frac{1}{\omega + \gamma\omega_{\text{pe}}} \right\} \\ & \leq \frac{M\omega_{\text{pe}}^2}{\pi c^3} \sqrt{\frac{2}{\pi}} \omega_{\text{pe}}^{-\frac{3}{2}} (t-T)^{-\frac{3}{2}} (1 - c_1^2/c^2)^{-\frac{3}{4}} \frac{\omega}{\omega^2 - \gamma^2\omega_{\text{pe}}^2}. \end{aligned}$$

We also note that, according to (3.35), the quantity γ is bounded: $\gamma = \frac{\omega_{\text{pe}}(t-T)}{y(T, t, \mathbf{x})} \leq \frac{1}{\sqrt{1 - c_1^2/c^2}}$. Then, assuming that $\omega \gg \omega_{\text{pe}}$, we drop the quadratic term $\mathcal{O}(\frac{\gamma^2\omega_{\text{pe}}^2}{\omega^2})$ and get

$$(3.38) \quad |\varphi_2(\mathbf{x}, t)| \leq \frac{M}{\pi c^3} \sqrt{\frac{2}{\pi}} \omega_{\text{pe}}^{-\frac{1}{2}} (t-T)^{-\frac{3}{2}} (1 - c_1^2/c^2)^{-\frac{3}{4}} \frac{\omega_{\text{pe}}}{\omega}.$$

Estimate (3.38) for the correction φ_2 is valid inside the lacuna of the wave equation in a narrower cone $|\mathbf{x}| < c(t - T) - \delta(t) = c_1(t - T)$. As before, the magnitude of the correction φ_2 now needs to be compared against the magnitude of the solution φ_1 inside the wave packet. For the purpose of comparison, we will consider φ_1 given by (3.26) on the boundary of the lacuna, i.e., exactly at the aft front $|\mathbf{x}| = c(t - T)$:

$$\varphi_1(\mathbf{x}, t) = \frac{M}{4\pi c^3} \frac{\sin(\omega T)}{t - T}.$$

Using estimate (3.38), we can therefore write (cf. formula (3.31))

$$(3.39) \quad \frac{\sup |\varphi_2|}{\sup |\varphi_1|} = \mathcal{O} \left(\omega_{pe}^{-\frac{1}{2}} (t - T)^{-\frac{1}{2}} \frac{\omega_{pe}}{\omega} \right).$$

From estimate (3.39) we see not only that for long propagation times the depth of a weak lacuna is controlled by the ratio $\frac{\omega_{pe}}{\omega}$ (similar to the case of short times) but that it also decays with the rate proportional to the inverse square root of time. We need to remember, however, that whereas in the previous estimate (3.31) we could use the maximum of the residual field φ_2 all across the lacuna $|\mathbf{x}| < c(t - T)$, in estimate (3.39) it can be taken only across a narrower cone $|\mathbf{x}| < c(t - T) - \delta(t) = c_1(t - T)$; see formula (3.35).

Let us additionally note that if we were to allow regions wider than the cone $|\mathbf{x}| < c_1(t - T)$ when analyzing the rate of growth of y , i.e., if we were to take the gap width $\delta(t)$ increasing more slowly than $(c - c_1)(t - T)$ (see formula (3.34)), then we would still obtain the key quantification of the depth of the weak lacuna by means of $\frac{\omega_{pe}}{\omega}$, but we could lose the additional decay $\sim \omega_{pe}^{-\frac{1}{2}} (t - T)^{-\frac{1}{2}}$ for long propagation times. For example, let $\delta(t) = A(t - T)^{\frac{1}{3}}$, where A is an appropriate constant needed to take into account that t is time and δ is distance. Then, for large times t we would obviously have $\delta^2(t) \ll 2c(t - T)\delta(t)$ and, consequently, $y = \frac{\omega_{pe}}{c} \sqrt{2c(t - T)\delta - \delta^2} \approx \frac{\omega_{pe}}{c} \sqrt{2cA}(t - T)^{\frac{2}{3}}$. In other words, instead of (3.35) we obtain

$$(3.40) \quad \forall \mathbf{x} : |\mathbf{x}| \leq c(t - T) - A(t - T)^{\frac{1}{3}} \quad \& \quad \forall \tau \in [0, T] : \\ y(\tau, t, \mathbf{x}) \geq y(T, t, \mathbf{x}) \gtrsim \frac{\omega_{pe}}{c} \sqrt{2cA}(t - T)^{\frac{2}{3}}.$$

Accordingly, estimate (3.38) gets replaced by

$$(3.41) \quad |\varphi_2(\mathbf{x}, t)| \leq \frac{M}{2\pi c^3} \sqrt{\frac{2}{\pi}} \omega_{pe}^{-\frac{1}{2}} (t - T)^{-1} \left(\frac{2A}{c} \right)^{-\frac{3}{4}} \frac{\omega_{pe}}{\omega},$$

and instead of (3.39) we obtain a simpler relation (cf. formula (3.31)):

$$(3.42) \quad \frac{\sup |\varphi_2|}{\sup |\varphi_1|} = \mathcal{O} \left(\frac{\omega_{pe}}{\omega} \right).$$

Clearly, estimate (3.39) guarantees a deeper lacuna for large times t than estimate (3.42) does. However, estimate (3.42) is valid on the region $|\mathbf{x}| < c(t - T) - A(t - T)^{\frac{1}{3}}$, which is wider than the cone $|\mathbf{x}| < c_1(t - T)$, $c_1 < c$, on which estimate (3.39) holds.

We should reemphasize, however, that both estimates (3.31) and (3.39) (as well as (3.42)) are only asymptotic results, for the small and large values, respectively, of the argument y of the Bessel function J_1 in formula (3.24). To corroborate and further expand the scope of these results, we will evaluate the convolution (3.24) numerically.

TABLE 3.1
The depth of the weak lacuna for different moments of time.

$\frac{\omega_{pe}}{\omega}$	$\frac{1}{10}$	$\frac{1}{20}$	$\frac{1}{40}$	$\frac{1}{80}$
$t = 0.8$	$1.16 \cdot 10^{-3}$	$4.57 \cdot 10^{-4}$	$1.95 \cdot 10^{-4}$	$1.01 \cdot 10^{-4}$
$t = 4$	$7.64 \cdot 10^{-2}$	$3.96 \cdot 10^{-2}$	$2.0 \cdot 10^{-2}$	$1.04 \cdot 10^{-2}$
$t = 10$	$3.87 \cdot 10^{-1}$	$1.98 \cdot 10^{-1}$	$1.04 \cdot 10^{-1}$	$5.43 \cdot 10^{-2}$
$t = 20$	$1.04 \cdot 10^0$	$4.88 \cdot 10^{-1}$	$2.47 \cdot 10^{-1}$	$1.35 \cdot 10^{-1}$

This is done using the Simpson rule on a very fine grid of the argument τ in order to guarantee that the level of the truncation error is far below the magnitude of either φ_1 or φ_2 . To provide a most transparent interpretation of the numerical results, we also adopt a slightly different notion of the depth of a weak lacuna, namely, $\frac{\max |\varphi_{\text{lacuna}}|}{\max |\varphi_{\text{packet}}|}$, where $\varphi_{\text{lacuna}} = \varphi_2$ and $\varphi_{\text{packet}} = \varphi_1 + \varphi_2$. This new definition immediately provides a quantitative measure of how big the residual field inside the lacuna is compared to the total field inside the wave packet. For computations, we select $\omega_{pe} = 1$, $T = 2\pi/10$, and in Table 3.1 present the depth of the weak lacuna for different values of ω_{pe}/ω and different moments of time t .

From Table 3.1, one can clearly see that for all moments of time—small, intermediate (not covered by the asymptotics), and large—the depth of the weak lacuna is indeed proportional to the quantity ω_{pe}/ω . However, the maximum of the contaminating field φ_2 is taken in Table 3.1 across the entire lacuna $|\mathbf{x}| < c(t - T)$. Therefore, as expected, we do not observe any decay of the depth as the time increases; we rather observe the increase. In fact, this increase is due to the “tail” of the residual field that decays toward the center of the lacuna, as shown in Figure 3.1.

On the other hand, if we were to take a region narrower than the cone $|\mathbf{x}| < c(t - T)$ to evaluate the depth of the weak lacuna, then we would be able to actually see its decrease in time, as prescribed previously by the asymptotic estimates. In Table 3.2, we present the same quantity as in Table 3.1, except that $\max |\varphi_{\text{lacuna}}| = \max |\varphi_2|$ is evaluated on a narrower cone $|\mathbf{x}| < c_1(t - T)$, where $c_1 = 0.75c$; see formula (3.35). The time range in Table 3.2 covers only intermediate to large intervals. From Table 3.2, one can clearly see not only that the depth of the weak lacuna is inversely proportional to ω_{pe}/ω for every particular moment of time, but that it also decays roughly as the inverse square root of time for every particular value of ω_{pe}/ω ; see formula (3.39).

An intermediate conclusion that we can draw, based on the combined use of asymptotic arguments and numerical quadratures, is that for high-frequency transverse electromagnetic waves that propagate in a dilute isotropic plasma (with particular pointwise excitation) one can still observe lacunae in the solutions but only in an approximate sense. The depth of these approximate, or weak, lacunae is proportional to the ratio of the Langmuir frequency of the plasma over the primary carrier frequency of the waves.

3.5. Numerical tests. In this section, we report on some results enabled by exploiting the weak lacunae in the computational context. As of yet, these results do not amount to a systematic numerical study. They rather provide a proof-of-concept illustration, whereas a broader and more coherent account of numerical simulations will be reported later.

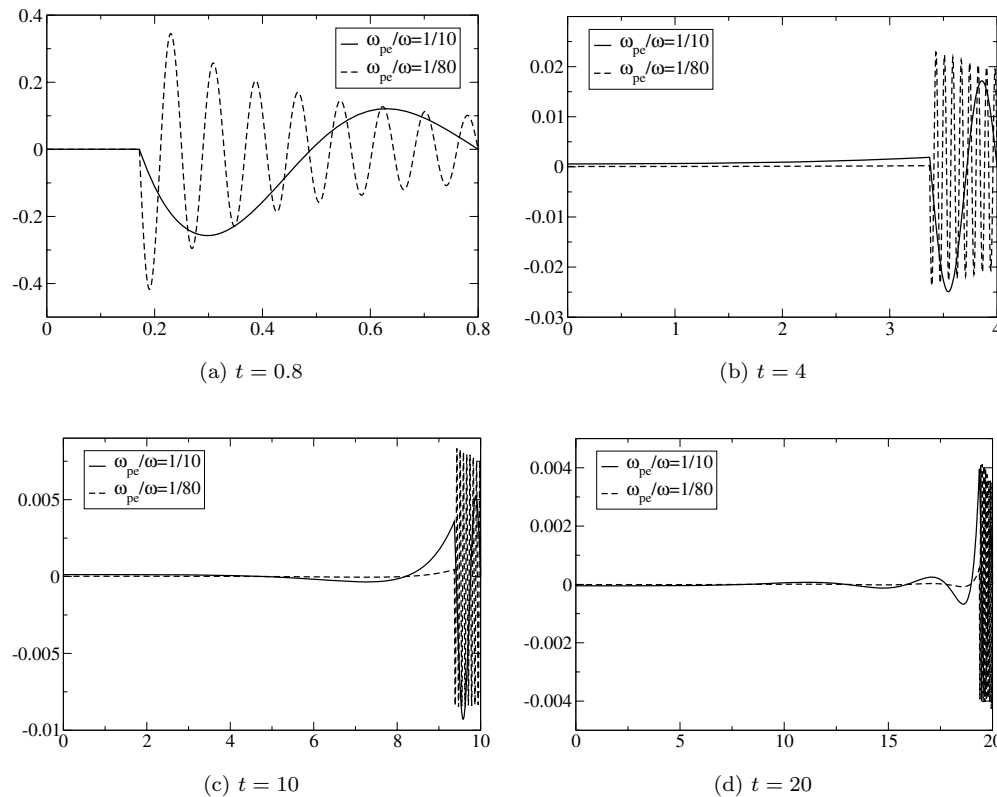


FIG. 3.1. Solution of the Klein–Gordon equation inside the lacuna and inside the wave packet.

TABLE 3.2
The depth of a weak lacuna for $c_1 = 0.75c$ and different moments of time.

$\frac{\omega_{pe}}{\omega}$	$\frac{1}{10}$	$\frac{1}{20}$	$\frac{1}{40}$	$\frac{1}{80}$
$t = 4$	$4.80 \cdot 10^{-2}$	$2.48 \cdot 10^{-2}$	$1.26 \cdot 10^{-2}$	$6.52 \cdot 10^{-3}$
$t = 10$	$3.64 \cdot 10^{-2}$	$1.81 \cdot 10^{-2}$	$9.47 \cdot 10^{-3}$	$4.93 \cdot 10^{-3}$
$t = 20$	$3.14 \cdot 10^{-2}$	$1.33 \cdot 10^{-2}$	$6.56 \cdot 10^{-3}$	$3.56 \cdot 10^{-3}$

We apply the lacunae-based algorithm of [24] to the Klein–Gordon equation (3.19). The algorithm of [24] was originally developed for the d’Alembert equation. It yields nonlocal ABCs that enable the computation of an unsteady wave field on a given finite region of interest. The rest of the space beyond this finite computational region is truncated, and the ABCs provide the required closure at the external artificial boundary so that the outgoing waves can propagate without any nonphysical reflections. Our objective hereafter is to demonstrate that the weak lacunae of section 3.4 can sometimes substitute for the actual lacunae in the numerical framework.

Lacunae-based ABCs for the genuine diffusionless case are constructed in two stages. Below we provide only a very brief description of the method and refer the reader to [24, 25] for details. A key initial assumption is that the overall infinite-domain problem has a unique solution and that (at least) outside of the aforementioned

finite region of interest this solution is governed by a linear homogeneous equation, such as the d'Alembert equation. At the first stage, the original problem is decomposed into two subproblems that depend on one another. The interior subproblem is formulated on the bounded computational domain. It inherits all the structure and properties of the original problem on this domain. As the computational domain is obtained by truncation, the interior subproblem obviously requires a closure, i.e., the ABCs, at the outer boundary. The ABCs are to be provided by the solution of the exterior subproblem. The latter, in turn, is formulated on the entire space and is driven by the special auxiliary sources that depend on the solution of the interior problem. The governing equation for the exterior subproblem on the entire space is the same linear homogeneous equation that governs the solution of the original problem outside the region of interest.

At the second stage, the two problems are integrated concurrently. In doing so, the algorithm for integrating the exterior problem is built around the presence of lacunae. The continuously operating auxiliary sources are partitioned in time into finite fragments. The solution due to each fragment has a lacuna, and the entire domain of interest falls inside this lacuna after a predetermined interval of time. Once this happens, the computation for this particular fragment does not need to be continued any further. Moreover, no wave can travel more than a certain fixed distance away from the source during this interval of time, which implies that the computations can always be conducted on a bounded auxiliary domain of a fixed nonincreasing size. This is the mechanism of transition from an infinite-domain formulation to a finite-domain one. Altogether, one can show that at any given moment of time only a finite fixed number of fragments contribute to the solution of the exterior problem, and each contribution needs to be computed only over a fixed time interval. This yields the exact unsteady ABCs with only fixed and limited extent of nonlocality in time. The performance of these ABCs does not deteriorate when integrating over long time intervals [24].

Replacing genuine lacunae by weak lacunae in the framework of the ABC algorithm basically means that the interior problem is still integrated in its entirety, whereas the dispersive effects for the exterior problem, i.e., for the boundary conditions, are artificially “cut short.” Indeed, for each element of the source partition the solution to the exterior problem is computed only until the region of interest falls inside the lacuna. The effect of the corresponding mismatch on the overall numerical performance will be thoroughly studied in the future. In the meantime, we simply provide some computational examples.

We are solving a model problem of radiation of waves by a known source. The exact solution for this problem is available; it is obtained by reverse engineering, i.e., by picking a function, substituting it under the differential operator, and deriving the right-hand side. For actual computations, we choose the Yee scheme [36], which is a well-known staggered central-difference scheme that has second order accuracy. We also set $\omega_{pe}/\omega = 1/100$ and select other parameters (grids, geometry, etc.) as in [24]. Namely, the computations are conducted on a uniform grid in the cylindrical coordinates. The methodology does not require that the grid be fitted to the shape of the domain of interest, and we choose the latter spherical. Note that the parameter c_1 (see formulae (3.34) and (3.35)), is not specified explicitly as input for the computational procedure, but other parameters are specified so as to effectively make it $c_1/c \approx 0.9$.

In Figure 3.2, we present the results of the grid convergence study (binary logarithm of the maximum norm of the error as a function of time) for two different values of the diameter of the sphere. The grid dimensions shown in Figure 3.2 pertain to the

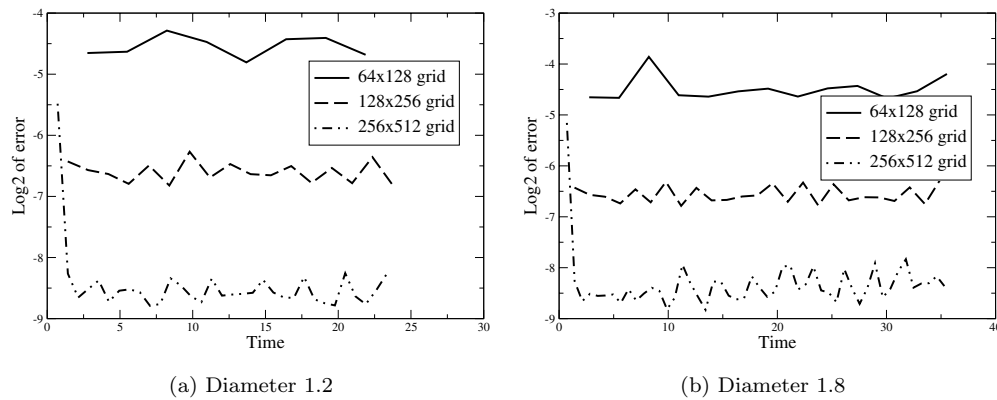


FIG. 3.2. Numerical performance of the ABCs based on weak lacunae.

auxiliary domain of cylindrical coordinates that has radius π and length 2π . The propagation speed is taken equal to one, and the computations are conducted over the time interval equivalent to 20 times the time required for the waves to travel across the sphere. At least for the particular setup selected, the plots in Figure 3.2 experimentally corroborate the design convergence rate of the scheme (second order) equipped with the ABCs based on the weak lacunae.

3.6. Anisotropic case. As has been mentioned, the primary source of anisotropy in the ionospheric plasma is the magnetic field of the Earth. It may play an important role for the propagation of electromagnetic waves. In particular, it may affect the structure and depth of the weak lacunae. In this section, we outline an approach to analyzing the weak lacunae in the presence of a constant external magnetic field.

Let $\mathbf{B}_0 = \text{const}$ be the magnetic field of the Earth. Then, the Lorentz term is to be kept on the right-hand side of (3.2), and instead of (3.3) we obtain

$$(3.43) \quad m_e \frac{d\mathbf{u}}{dt} = -e\mathbf{E} - \frac{e}{c} \mathbf{u} \times \mathbf{B}_0.$$

We now need to find the first time derivative of the induced current that provides the excitation for the electric field on the right-hand side of the governing equation (3.1). Substituting $\mathbf{j}_{\text{ind}} = -en_e \mathbf{u}$ into (3.43), we obtain

$$(3.44) \quad \dot{\mathbf{j}}_{\text{ind}} = \frac{\omega_{\text{pe}}^2}{4\pi} \mathbf{E} - \Omega_e \mathbf{j}_{\text{ind}} \times \frac{\mathbf{B}_0}{|\mathbf{B}_0|}.$$

Equation (3.44) is a first order ordinary differential equation with respect to the unknown current \mathbf{j}_{ind} , which is a function of time. It needs to be solved along with (3.1). It is clear that in doing so the dependence of $\dot{\mathbf{j}}_{\text{ind}}$ on \mathbf{E} will be given by a convolution, which means that the responses of the anisotropic medium (3.43) will, generally speaking, be nonlocal in time. Later in the section we will see, however, that under certain assumptions the effect of anisotropy can still be regarded as small.

We begin with providing an elementary frequency-domain analysis. The use of the variable \mathbf{P} (polarization), where $\dot{\mathbf{j}}_{\text{ind}} = \frac{\partial \mathbf{P}}{\partial t}$, will be more convenient on some occasions, because it has the same dimension as the field \mathbf{E} . In the frequency domain,

(3.44) can be transformed into

$$(3.45) \quad \omega^2 \mathbf{P}(\omega) + i\omega\Omega_e \mathbf{P}(\omega) \times \frac{\mathbf{B}_0}{|\mathbf{B}_0|} = -\frac{\omega_{pe}^2}{4\pi} \mathbf{E}(\omega).$$

Assuming with no loss of generality that the magnetic field \mathbf{B}_0 is aligned with the Cartesian coordinate z , we solve (3.45) with respect to $\mathbf{P}(\omega)$ and obtain

$$(3.46) \quad \mathbf{P}(\omega) = -\frac{\omega_{pe}^2}{4\pi\omega^2} \mathbf{E}(\omega) + \frac{\omega_{pe}^2}{4\pi\omega^2} \frac{i\omega\Omega_e}{\omega^2 - \Omega_e^2} \mathbf{E}(\omega) \times \frac{\mathbf{B}_0}{|\mathbf{B}_0|} - \frac{\omega_{pe}^2}{4\pi\omega^2} \frac{\Omega_e^2}{\omega^2 - \Omega_e^2} \begin{bmatrix} 1 & 0 & 0 \\ 0 & 1 & 0 \\ 0 & 0 & 0 \end{bmatrix} \mathbf{E}(\omega).$$

Note that the first term on the right-hand side of (3.46) is exactly the same as we obtained in the isotropic case; see formula (3.5). The second and third terms on the right-hand side of (3.46) are due to the presence of the magnetic field \mathbf{B}_0 . These terms, which are proportional to the first and second power of the cyclotron frequency Ω_e , respectively, are known to be responsible for the effects of gyrotropy and Faraday rotation that accompany the propagation of electromagnetic waves in the anisotropic plasma; see [18, 21].

The case of particular interest for us is that of the high-frequency propagation. If $\omega \gg \omega_{pe}$, then also $\omega \gg \Omega_e$, because according to section 3.1, Ω_e is about an order of magnitude lower than ω_{pe} for the typical range of parameters that characterize the ionospheric plasma. Consequently, instead of (3.46) we can write

$$(3.47) \quad \mathbf{P}(\omega) \approx -\frac{\omega_{pe}^2}{4\pi\omega^2} \mathbf{E}(\omega) + \frac{\omega_{pe}^2}{4\pi\omega^2} \frac{i\Omega_e}{\omega} \mathbf{E}(\omega) \times \frac{\mathbf{B}_0}{|\mathbf{B}_0|}.$$

Note that $\mathbf{B}_0/|\mathbf{B}_0|$ on the right-hand side of (3.47) is a dimensionless unit vector in the direction of the magnetic field \mathbf{B}_0 . Then, by comparing the two terms on the right-hand side of (3.47) and by recalling that the effect of the first term on lacunae back in the time domain is $\mathcal{O}(\frac{\omega_{pe}}{\omega})$ (see estimates (3.31) and (3.39)), we can qualitatively conjecture that the additional effect of anisotropy on lacunae is likely to be $\mathcal{O}(\frac{\omega_{pe}}{\omega} \cdot \sqrt{\frac{\Omega_e}{\omega}})$. It is expected to be much smaller than the $\mathcal{O}(\frac{\omega_{pe}}{\omega})$ attributed to the “primary” dispersion, because the extra factor contained in the second term on the right-hand side of (3.47) is $\Omega_e/\omega \ll 1$.

To conduct the analysis in the time domain, we employ the Laplace transform instead of the Fourier transform and, assuming homogeneous initial conditions for the polarization, obtain (cf. formula (3.45))

$$(3.48) \quad s^2 \mathbf{P}(s) + s\Omega_e \mathbf{P}(s) \times \frac{\mathbf{B}_0}{|\mathbf{B}_0|} = \frac{\omega_{pe}^2}{4\pi} \mathbf{E}(s).$$

The primary quantity of interest for us is $s^2 \mathbf{P}$, because $\mathbf{j}'_{\text{ind}} = \mathbf{P}''$, and we find

$$s^2 \mathbf{P}(s) = \frac{\omega_{pe}^2}{4\pi} \mathbf{E}(s) + \frac{\omega_{pe}^2}{4\pi} \begin{bmatrix} -\frac{\Omega_e^2}{s^2 + \Omega_e^2} & -\frac{\Omega_e s}{s^2 + \Omega_e^2} & 0 \\ \frac{\Omega_e s}{s^2 + \Omega_e^2} & -\frac{\Omega_e^2}{s^2 + \Omega_e^2} & 0 \\ 0 & 0 & 0 \end{bmatrix} \mathbf{E}(s).$$

Consequently,

$$\begin{aligned}(j'_{\text{ind}})_x &= P''_x = \frac{\omega_{\text{pe}}^2}{4\pi} E_x + \frac{\omega_{\text{pe}}^2 \Omega_e}{4\pi} [-\sin(\Omega_e t) * E_x(t) - \cos(\Omega_e t) * E_y(t)], \\(j'_{\text{ind}})_y &= P''_y = \frac{\omega_{\text{pe}}^2}{4\pi} E_y + \frac{\omega_{\text{pe}}^2 \Omega_e}{4\pi} [\cos(\Omega_e t) * E_x(t) - \sin(\Omega_e t) * E_y(t)], \\(j'_{\text{ind}})_z &= P''_z = \frac{\omega_{\text{pe}}^2}{4\pi} E_z.\end{aligned}$$

From the previous expressions we see that electromagnetic responses of the anisotropic plasma involve off-diagonal terms, i.e., relate different components of the field and current vectors (as opposed to only respective components). Therefore, we will employ diagonalization by means of the transformation \mathcal{T} :

$$\mathcal{T} = \begin{bmatrix} i & -i & 0 \\ 1 & 1 & 0 \\ 0 & 0 & 1 \end{bmatrix}, \quad \mathcal{T}^{-1} = \begin{bmatrix} -i/2 & 1/2 & 0 \\ i/2 & 1/2 & 0 \\ 0 & 0 & 1 \end{bmatrix}.$$

Let $\mathbf{E} = \mathcal{T} \mathbf{G}$ and $\mathbf{P} = \mathcal{T} \mathbf{Q}$. Then, (3.48) transforms into

$$(3.49) \quad s^2 \mathbf{Q}(s) = \frac{\omega_{\text{pe}}^2}{4\pi} \mathbf{G}(s) + \frac{\omega_{\text{pe}}^2 \Omega_e}{4\pi} \frac{\Omega_e}{s^2 + \Omega_e^2} \begin{bmatrix} -\Omega_e + is & 0 & 0 \\ 0 & -\Omega_e - is & 0 \\ 0 & 0 & 0 \end{bmatrix} \mathbf{G}(s).$$

If we also define $\mathbf{j}_{\text{ind}} = \mathcal{T} \mathbf{q}$, then $s \mathbf{q}(s) = s^2 \mathbf{Q}(s)$, and from (3.49) we find

$$(3.50) \quad \begin{aligned}q'_x(t) &= \frac{\omega_{\text{pe}}^2}{4\pi} G_x(t) + i \frac{\omega_{\text{pe}}^2 \Omega_e}{4\pi} [e^{i\Omega_e t} * G_x(t)], \\q'_y(t) &= \frac{\omega_{\text{pe}}^2}{4\pi} G_y(t) - i \frac{\omega_{\text{pe}}^2 \Omega_e}{4\pi} [e^{-i\Omega_e t} * G_y(t)], \\q'_z(t) &= \frac{\omega_{\text{pe}}^2}{4\pi} G_z(t).\end{aligned}$$

To quantify the effect of anisotropy, we will need to analyze the convolutions on the right-hand side of the first two equations (3.50):

$$e^{\pm i\Omega_e t} * G_{x,y}(t) = \int_0^t e^{\pm i\Omega_e(t-v)} G_{x,y}(v) dv = e^{\pm i\Omega_e t} \int_0^t e^{\mp i\Omega_e v} G_{x,y}(v) dv.$$

Consider, for example, the component G_x and introduce the following ansatz: $G_x(v) = e^{i\omega t} \tilde{G}_x(v)$, where $\tilde{G}_x(v)$ is assumed to be a slowly varying function. Then, we integrate by parts twice and obtain

$$\begin{aligned}\int_0^t e^{-i\Omega_e v} G_x(v) dv &= \frac{1}{i(\omega - \Omega_e)} \left[G_x(t) e^{-i\Omega_e t} - \int_0^t e^{i(\omega - \Omega_e)v} \tilde{G}'_x(v) dv \right] \\&= \frac{1}{i(\omega - \Omega_e)} G_x(t) e^{-i\Omega_e t} + \frac{\tilde{G}'_x(t) e^{i(\omega - \Omega_e)t} - \tilde{G}'_x(0)}{(\omega - \Omega_e)^2} \\&\quad - \frac{1}{(\omega - \Omega_e)^2} \int_0^t e^{i(\omega - \Omega_e)v} \tilde{G}''_x(v) dv.\end{aligned}$$

Consequently,

$$(3.51) \quad \begin{aligned} \frac{\partial q_x}{\partial t} &= \frac{\omega_{\text{pe}}^2}{4\pi} G_x(t) + \frac{\omega_{\text{pe}}^2}{4\pi} \frac{\Omega_e}{\omega - \Omega_e} G_x(t) \\ &+ e^{i\Omega_e t} \frac{\omega_{\text{pe}}^2}{4\pi} \frac{\Omega_e}{\omega - \Omega_e} \frac{\tilde{G}'_x(t) e^{i(\omega - \Omega_e)t} - \tilde{G}'_x(0)}{\omega - \Omega_e} \\ &- e^{i\Omega_e t} \frac{\omega_{\text{pe}}^2}{4\pi} \frac{\Omega_e}{\omega - \Omega_e} \frac{1}{\omega - \Omega_e} \int_0^t e^{i(\omega - \Omega_e)v} \tilde{G}''_x(v) dv. \end{aligned}$$

Slow variation of $\tilde{G}_x(v)$ means that it is slow on the scale of the high-frequency oscillation ω , and in many cases this slowness is a natural assumption about the field. Under this assumption, the third and fourth terms on the right-hand side of equality (3.51) can be neglected. Indeed, the third term is small compared to the second one because

$$\frac{\max |G'_x|}{\omega - \Omega_e} \ll \max |G_x|.$$

As for the fourth term on the right-hand side of (3.51), using the Riemann–Lebesgue lemma we can write

$$\int_0^t e^{i(\omega - \Omega_e)v} \tilde{G}''_x(v) dv = o(\max |G''_x|) \quad \text{as } \omega \rightarrow \infty.$$

Therefore, for high carrier frequencies it is also small compared to the second term. Consequently,

$$(3.52) \quad \frac{\partial q_x}{\partial t} \approx \frac{\omega_{\text{pe}}^2}{4\pi} \left(1 + \frac{\Omega_e}{\omega - \Omega_e} \right) G_x(t),$$

and a similar expression can be obtained for q'_y . Hence, when the field is represented as the product of a rapidly oscillating carrier times a slowly varying envelope, the nonlocal responses due to the anisotropy can be approximated by local expressions of the type (3.52).

Finally, let us revisit the governing equation for the field (3.1). We note that when plasma becomes anisotropic, the notion of longitudinal and transverse waves often changes its meaning, and in the literature one would typically consider the waves that propagate along the magnetic field and those that propagate perpendicular to the magnetic field; see, e.g., [8]. Of course, other propagation angles are also possible, and, in general, the split into the longitudinal and transverse components is not always straightforward. We will, however, still consider the transverse field \mathbf{E}_\perp in the previous sense of the word, i.e., the one that satisfies $\text{div} \mathbf{E}_\perp = 0$. Let also $\mathbf{E}_\perp = \mathcal{T} \mathbf{G}$; then from (3.1) we obtain

$$\frac{\partial \mathcal{T} \mathbf{G}}{\partial t} - c^2 \Delta (\mathcal{T} \mathbf{G}) + 4\pi \frac{\partial \mathcal{T} \mathbf{q}}{\partial t} = \mathbf{0}.$$

Since \mathcal{T} is a constant matrix, and the vector Laplacian in the Cartesian coordinates applies independently to individual components, we can use formulae (3.50), (3.52) and write

$$\frac{\partial \mathbf{G}}{\partial t} - c^2 \Delta \mathbf{G} + \omega_{\text{pe}}^2 \begin{bmatrix} 1 + \frac{\Omega_e}{\omega - \Omega_e} & 0 & 0 \\ 0 & 1 + \frac{\Omega_e}{\omega - \Omega_e} & 0 \\ 0 & 0 & 1 \end{bmatrix} \mathbf{G} = \mathbf{0}.$$

This is a vector equation, which is equivalent to three scalar Klein–Gordon equations. For the first two components the dispersive term is $\sim \omega_{pe}^2 (1 + \frac{\Omega_e}{\omega - \Omega_e})$ as opposed to simply $\sim \omega_{pe}^2$, which was the case in section 3.4. We therefore conclude that the additional effect of anisotropy on weak lacunae of electromagnetic waves in the dilute ionospheric plasma can be approximately measured as $\mathcal{O}(\frac{\omega_{pe}}{\omega} \sqrt{\frac{\Omega_e}{\omega - \Omega_e}})$.

4. Discussion. Classical lacunae can be observed in the solutions of the Maxwell equations only when the electromagnetic waves propagate in vacuum or in dielectric media with static response. Otherwise, the propagation is accompanied by aftereffects, and there are no sharp aft fronts and no lacunae in the solutions. For low incident frequencies, the mechanism that destroys the lacunae can largely be attributed to dissipation due to the Ohm conductivity. For high incident frequencies, when the material coefficients can no longer be considered constant, the diffusion of waves is basically caused by the physical dispersion. However, for the propagation of transverse electromagnetic waves in dilute plasma, when the incident frequency is much higher than the Langmuir frequency, lacunae can still be identified in the corresponding solutions of the Maxwell equations, although in an approximate sense. The depth of these weak lacunae, i.e., the magnitude of the residual field relative to the magnitude of the field in the primary wave packet, is proportional to the ratio of the Langmuir frequency over the primary carrying frequency of the waves. In the anisotropic case, when the plasma is immersed into the external magnetic field, there is an additional small factor, approximately equal to the square root of the ratio of the cyclotron frequency over the carrier frequency, that affects the depth of the weak lacunae.

An interesting subject for future study could be analysis of the case when anisotropic responses should remain nonlocal in time, as well as a more careful analysis of the conductivity mechanisms in the ionosphere. On the numerical side, the future direction is the ABC algorithm based on the weak lacunae.

REFERENCES

- [1] M. F. ATIYAH, R. BOTT, AND L. GÄRDING, *Lacunae for hyperbolic differential operators with constant coefficients*. I, Acta Math., 124 (1970), pp. 109–189.
- [2] M. F. ATIYAH, R. BOTT, AND L. GÄRDING, *Lacunae for hyperbolic differential operators with constant coefficients*. II, Acta Math., 131 (1973), pp. 145–206.
- [3] M. BELGER, R. SCHIMMING, AND V. WÜNSCH, *A survey on Huygens' principle*, Z. Anal. Anwendungen, 16 (1997), pp. 9–36.
- [4] N. N. BOGOLIUBOV AND D. V. SHIRKOV, *Introduction to the Theory of Quantized Fields*, Interscience Monographs in Physics and Astronomy, Vol. III, Interscience, New York, London, 1959.
- [5] M. BORN AND E. WOLF, *Principles of Optics: Electromagnetic Theory of Propagation, Interference and Diffraction of Light*, 7th ed., Cambridge University Press, Cambridge, UK, 1999.
- [6] K. G. BUDDEN, *The Propagation of Radio Waves: The Theory of Radio Waves of Low Power in the Ionosphere and Magnetosphere*, Cambridge University Press, Cambridge, UK, 1985.
- [7] R. COURANT AND D. HILBERT, *Methods of Mathematical Physics*, Vol. II, Wiley, New York, 1962.
- [8] V. L. GINZBURG, *The Propagation of Electromagnetic Waves in Plasmas*, Internat. Ser. Monogr. Electromagnetic Waves 7, Pergamon Press, Oxford, UK, 1964.
- [9] P. GÜNTHER, *Ein Beispiel einer nichttrivialen Huygensschen Differentialgleichung mit vier unabhängigen Variablen*, Arch. Rational Mech. Anal., 18 (1965), pp. 103–106.
- [10] P. GÜNTHER, *Huygens' Principle and Hyperbolic Equations*, Perspect. Math. 5, Academic Press, Boston, 1988.
- [11] P. GÜNTHER, *Huygens' principle and Hadamard's conjecture*, Math. Intelligencer, 13 (1991), pp. 56–63.
- [12] J. HADAMARD, *Lectures on Cauchy's Problem in Linear Partial Differential Equations*, Yale University Press, New Haven, CT, 1923.

- [13] J. HADAMARD, *Problème de Cauchy*, Hermann, Paris, 1932.
- [14] J. HADAMARD, *The problem of diffusion of waves*, Ann. of Math. (2), 43 (1942), pp. 510–522.
- [15] B. B. KADOMTSEV, *Collective Phenomena in Plasma* [*Kollektivnye yavleniya v plazme*], 2nd ed., Nauka, Moscow, 1988 (in Russian).
- [16] J. E. LAGNESE AND K. L. STELLMACHER, *A method of generating classes of Huygens' operators*, J. Math. Mech., 17 (1967), pp. 461–472.
- [17] L. D. LANDAU AND E. M. LIFSHITZ, *Course of Theoretical Physics, Vol. 2, The Classical Theory of Fields*, 4th ed., Pergamon Press, Oxford, UK, 1975.
- [18] L. D. LANDAU AND E. M. LIFSHITZ, *Course of Theoretical Physics, Vol. 8, Electrodynamics of Continuous Media*, Pergamon International Library of Science, Technology, Engineering and Social Studies, Pergamon Press, Oxford, 1984.
- [19] P. D. LAX AND R. S. PHILLIPS, *An example of Huygens' principle*, Comm. Pure Appl. Math., 31 (1978), pp. 415–421.
- [20] M. MATTHISSON, *Le problème de Hadamard relatif à la diffusion des ondes*, Acta Math., 71 (1939), pp. 249–282.
- [21] D. B. MELROSE AND R. C. MCPHEDRAN, *Electromagnetic Processes in Dispersive Media. A Treatment Based on the Dielectric Tensor*, Cambridge University Press, Cambridge, UK, 1991.
- [22] P. M. MORSE AND H. FESHBACH, *Methods of Theoretical Physics* (2 volumes), Internat. Ser. Pure Appl. Phys., McGraw–Hill, New York, 1953.
- [23] I. PETROWSKY, *On the diffusion of waves and the lacunas for hyperbolic equations*, Rec. Math. [Mat. Sbornik] N.S. 17 (1945), pp. 289–370.
- [24] V. S. RYABEN'KII, S. V. TSYNKOV, AND V. I. TURCHANINOV, *Global discrete artificial boundary conditions for time-dependent wave propagation*, J. Comput. Phys., 174 (2001), pp. 712–758.
- [25] V. S. RYABEN'KII, S. V. TSYNKOV, AND V. I. TURCHANINOV, *Long-time numerical computation of wave-type solutions driven by moving sources*, Appl. Numer. Math., 38 (2001), pp. 187–222.
- [26] R. SCHIMMING, *A review of Huygens' principle for linear hyperbolic differential equations*, in Proceedings of the IMU Symposium Group-Theoretical Methods in Mechanics, Novosibirsk, USSR, 1978, USSR Academy of Science, Siberian Branch, Novosibirsk, Russia, 1978.
- [27] L. I. SEDOV, *Mechanics of Continuous Media*, Vols. 1 and 2, Ser. Theoret. Appl. Mech. 4, World Scientific, River Edge, NJ, 1997.
- [28] K. L. STELLMACHER, *Ein Beispiel einer Huyghensschen Differentialgleichung*, Nachr. Akad. Wiss. Göttingen Math.-Phys. Kl., Math.-Phys.-Chem. Abt., 1953 (1953), pp. 133–138.
- [29] K. L. STELLMACHER, *Eine Klasse huyghenscher Differentialgleichungen und ihre Integration*, Math. Ann., 130 (1955), pp. 219–233.
- [30] S. V. TSYNKOV, *Numerical solution of problems on unbounded domains. A review*, Appl. Numer. Math., 27 (1998), pp. 465–532.
- [31] S. V. TSYNKOV, *Artificial boundary conditions for the numerical simulation of unsteady acoustic waves*, J. Comput. Phys., 189 (2003), pp. 626–650.
- [32] S. V. TSYNKOV, *Artificial Boundary Conditions for the Numerical Simulation of Unsteady Electromagnetic Waves*, Tech. report CRSC-TR03-19, Center for Research in Scientific Computation, North Carolina State University, Raleigh, NC, 2003.
- [33] S. V. TSYNKOV, *Lacunae-based artificial boundary conditions for the numerical simulation of unsteady waves governed by vector models*, in Mathematical and Numerical Aspects of Wave Propagation—WAVES 2003 (Jyväskylä, Finland, 2003), G. C. Cohen, E. Heikkola, P. Joly, and P. Neittaanmäki, eds., Springer, Berlin, 2003, pp. 103–108.
- [34] S. V. TSYNKOV, *On the application of lacunae-based methods to Maxwell's equations*, J. Comput. Phys., 199 (2004), pp. 126–149.
- [35] E. T. WHITTAKER AND G. N. WATSON, *A Course of Modern Analysis. An Introduction to the General Theory of Infinite Processes and of Analytic Functions: With an Account of the Principal Transcendental Functions*, 4th ed., Cambridge University Press, New York, 1962.
- [36] K. S. YEE, *Numerical solution of initial boundary value problem involving Maxwell's equations in isotropic media*, IEEE Trans. Antennas and Propagation, 14 (1966), pp. 302–307.